Zoonotic visceral leishmaniasis transmission: modeling, backward bifurcation, and optimal control

Article *in* Journal of Mathematical Biology · April 2016

DOI: 10.1007/s00285-016-0999-z

6 authors, including:

Songnian Zhao
Kansas State University
18 PUBLICATIONS **46** CITATIONS
SEE PROFILE

Yan Kuang
Kansas State University
14 PUBLICATIONS **32** CITATIONS
SEE PROFILE

Chih-Hang John Wu
Kansas State University
149 PUBLICATIONS **1,280** CITATIONS
SEE PROFILE

David Ben-Arieh
Kansas State University
124 PUBLICATIONS **1,703** CITATIONS
SEE PROFILE

J. Math. Biol.
DOI 10.1007/s00285-016-0999-z

Mathematical Biology

Zoonotic visceral leishmaniasis transmission: modeling, backward bifurcation, and optimal control

Songnian Zhao[1] · Yan Kuang[2] · Chih-Hang Wu[3] · David Ben-Arieh[4] · Marcelo Ramalho-Ortigao[5] · Kaiming Bi[6]

Received: 26 February 2015 / Revised: 16 March 2016

Abstract Visceral leishmaniasis (VL), a vector-borne disease caused by protozoan flagellates of the genus Leishmania, is transmitted by sand flies. After malaria, VL is the second-largest parasitic killer, responsible for an estimated 500,000 infections

✉ Chih-Hang Wu
chw@ksu.edu

Songnian Zhao
songnian@ksu.edu

Yan Kuang
ykuang@ksu.edu

David Ben-Arieh
davidbe@ksu.edu

Marcelo Ramalho-Ortigao
mortigao@ksu.edu

Kaiming Bi
bikaiming@ksu.edu

1 Department of Industrial and Manufacturing Systems Engineering, Kansas State University, 2022 Durland Hall, Manhattan, KS 66506, USA

2 Department of Industrial and Manufacturing Systems Engineering, Kansas State University, 2010 Durland Hall, Manhattan, KS 66506, USA

3 Department of Industrial and Manufacturing Systems Engineering, Kansas State University, 2018 Durland Hall, Manhattan, KS 66506, USA

4 Department of Industrial and Manufacturing Systems Engineering, Kansas State University, 2016 Durland Hall, Manhattan, KS 66506, USA

5 Department of Entomology, Kansas State University, 106 Waters Annex, Manhattan, KS 66506, USA

6 Department of Industrial and Manufacturing Systems Engineering, Kansas State University, 2032 Durland Hall, Manhattan, Kansas 66506, USA

Published online: 15 April 2016

and 51,000 deaths annually worldwide. Mathematical models proposed for VL have included the impact of dogs versus wild canids in disease dissemination and models developed to assist in control approaches. However, quantitative conditions that are required to control or eradicate VL transmission are not provided and there are no mathematical methods proposed to quantitatively calculate optimal control strategies for VL transmission. The research objective of this work was to model VL disease transmission system (specifically Zoonotic VL), perform bifurcation analysis to discuss control conditions, and calculate optimal control strategies. Three time-dependent control strategies involving dog populations, sand fly population, and humans are mainly discussed. Another strategy sometimes used in attempts to control zoonotic VL transmission, dog culling, is also evaluated in this paper.

Keywords Visceral leishmaniasis · Zoonotic disease transmission · Backward bifurcation · Optimal control

Mathematics Subject Classification 92B05 · 34H05 · 34H20

1 Introduction

Visceral leishmaniasis (VL) is a protozoan disease caused by parasites of the genus Leishmania and transmitted through the bite of infected sand flies. After malaria, VL is the second-largest parasitic killer in the world, occurring in 65 countries with a majority (90 %) of cases in poor rural and suburban areas of Bangladesh, India, Nepal, Sudan, Ethiopia, and Brazil. The current annual estimate of VL mortality is more than 50,000 (Desjeux 2004), an assumed underestimation because not all cases are reported and VL is often undiagnosed or unrecognized. VL has been become one of the most prevalent public health concerns because of its high morbid mortality. It is generally characterized by an acute stage with generalized symptoms, including fever, cachexia, hepatomegaly, splenomegaly, and pancytopenia.

VL can be classified into zoonotic visceral leishmaniasis (ZVL) and anthroponotic visceral leishmaniasis (AVL). ZVL is caused by *Leishmania infantum* transmitted by the bite of an infected sand fly from sylvatic animal reservoir (such as wild canids and rodents, or domestic, such as the domestic dog) to humans. ZVL is widely distributed from the Mediterranean Basin, parts of the Middle East and North Africa, and the Americas. Since the early 2000s, an outbreak of ZVL also has been identified in American Foxhounds in the United States (Rosypal et al. 2003). In contrast, AVL can be transmitted directly from humans to humans by the bite of an infected sand fly (Chappuis et al. 2007). AVL is found primarily in India (Bihar State) and other parts of the Indian Subcontinent (Stauch et al. 2011), and in Sudan and South Sudan and caused by *Leishmania donovani* (Jamjoom et al. 2004). Once a person is infected, the parasite migrates to internal organs such as the liver, spleen (hence "visceral"), and bone marrow. Lack of treatment almost always results in death of the host.

Several mathematical models have been constructed to describe VL transmission. Stauch et al. (2011) modeled the spread of VL in the Indian Subcontinent by modified SEIR model in terms of AVL characteristics and extended it to a ZVL model with

animal reservoirs. Vector-related intervention was recommended in combination with treatment-related intervention in order to control VL transmission. Ribas et al. (2013) used a mathematical model adapted from one proposed by Burattini et al. (1998) to assess interaction between humans, sand flies, and dogs. The risk of requiring the infection R was calculated and optimal control strategy was estimated based on the formula of calculating R. It provided a combination of two ways to control ZVL transmission instead of culling seropositive dogs: insecticide-impregnate collar and vector control. However, they fail to provide a quantitative condition to control or eradicate VL transmission and did not propose mathematical methods to quantitatively calculate optimal control strategies.

In this paper, a mathematical model was developed to describe the ZVL transmission process in Brazil using a modified SEIR model, particularly focused on the reservoir(dogs) because of the crucial role played by these animals in disease transmission. Castillo-Chavez and Song (2004) suggested that the zoonotic disease model may exhibit backward bifurcation, in which local asymptotically stable disease free equilibrium(DFE) co-exists with a locally-asymptotically stable endemic equilibrium when $R_0 < 1$. Using the reasonable range for each parameter in our mathematical model, a backward bifurcation analysis was performed, resulting in the conclusion that backward bifurcation may exhibit in ZVL transmission. In this case, the condition $R_0 < 1$ may lead to an endemic equilibrium instead of DFE. Therefore, $R_0 < 1$, the classical requirement for the control of infectious disease spread, although necessary, is no longer sufficient for ZVL elimination. Another significant parameter, R_c, was calculated, thereby demonstrating that it coexists in two equilibrium, disease-free equilibrium and endemic equilibrium, when $R_c < R_0 < 1$. In addition, optimal control was discussed to give support in decision for controlling disease transmission. A general mathematical method was used to analyze optimal control strategies and numerical analysis was described to illustrate implementation of this method. Based on numerical results, optimal control strategies are discussed.

The structure of this paper is as follows: Sect. 2 details a new mathematical model for ZVL transmission; Sect. 3 demonstrates the phenomenon of backward bifurcation existing in the model; Sect. 4 calculates optimal control strategies based on Pontryagins maximum principle and discusses impacts to disease control with various control costs and effectiveness of control strategies; Sect. 5 concludes the paper and suggests future work.

2 Mathematical model

In this section, a basic model for ZVL transmission dynamics among dogs-sand flies-humans system is constructed. Parameters used in the model are listed in Table 1.

ZVL is transmitted by female sand flies, with *Lutzomyia longipalpis* being the primary vector in the Americas. In this paper, we use the word "sand flies", primarily indicating *L. longipalpis* and other species of sand flies which are not ZVL vectors are not considered. Dogs serve as the primary reservoir host for the transmission of parasites to humans [dead-end hosts for ZVL (Hartemink et al. 2011)], and dogs are the principal risk factor for human infections with ZVL in endemic areas (Dantas-Torres

Table 1 Parameters in the model

Parameters	Interpretation
λ_d	Recruitment rate of susceptible dogs
λ_f	Recruitment rate of susceptible sand flies
λ_h	Recruitment rate of susceptible humans
$1/\mu_d$	Average lifespan of dogs
$1/\mu_f$	Average lifespan of sand flies
$1/\mu_h$	Average lifespan of humans
b_{fd}	Average biting rate per infected sand fly to dogs
b_{fh}	Average biting rate per infected sand fly to humans
β_{fd}	Transmission probability from an infected sand fly to a susceptible dog
β_{df}	Transmission probability from an infected dog to a susceptible sand fly
β_{fh}	Transmission probability from an infected sand fly to a susceptible human
d_d	VL-induced death rate of dogs (including culled dogs)
d_f	VL-induced death rate for sand flies
d_I	VL-induced death rate of humans
d_H	Death rate of hospitalized humans
m_f	Migration rate of sand flies
$1/\tau_d$	Incubation period in dogs
$1/\tau_f$	Incubation period in sand flies
$1/\tau_h$	Incubation period in humans
δ_h	Hospitalization rate of humans
r_d	Recovery rate of infected dogs
r_I	Natural recovery rate of infected humans
r_H	Recovery rate of hospitalized humans

and Brandão-Filho 2006; Courtenay et al. 2002). A system diagram of ZVL transmission among dogs, sand flies, and humans is shown in Fig. 1 in which populations for the three systems are assumed to be homogenous. In addition, the recovered dog may be changed back to infectious dogs if they are removed from treatment (dotted line from R_d to I_d in Fig. 1). However, this process is not shown in our model and we assumed that all recovered dogs are always under treatment. For humans, recovered humans are not necessarily immune and may be re-infected, but there is now evidence that some level of immunity can be achieved. In this paper, we assume recovered individuals either obtain the immunity or prevent themselves from getting infected. In addition, the VL cannot be transmitted from human to human, sand flies or dogs, so this assumption will not affect the spread of the VL. Moreover, absent from the parameters is the potential replacement of culled dogs with young animals, which

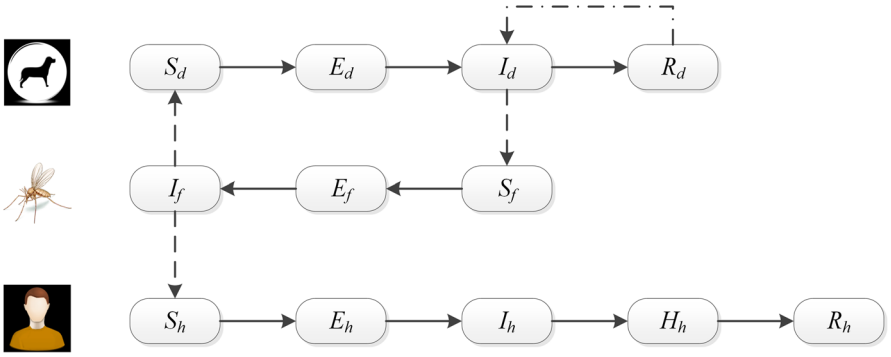

Fig. 1 System diagram of ZVL transmission model

is frequently adopted in many endemic areas, but are very hard to ascertain for the purpose of generality of the model.

In the above system, dogs were classified into four compartments: susceptible dogs (S_d), exposed/infected (but not infectious) dogs (E_d), infectious dogs (I_d), and recovered dogs (R_d). Susceptible dogs could be transferred to exposed dogs, exposed/infected dogs could be transferred to infectious dogs, and infectious dogs could recover and become recovered dogs. Similarly, sand flies were distributed among susceptible sand flies (S_f), exposed/infected sand flies (E_f), and infectious sand flies (I_f). A modified SEIR model for human system is defined as susceptible humans (S_h), exposed (during incubation period) humans (E_h), infected humans (I_h), hospitalized humans (H_h), and recovered humans (R_h). The mathematical model for three sub-systems is shown below.

2.1 Dog population

$$\frac{dS_d}{dt} = \lambda_d - \frac{b_{fd}\beta_{fd}I_f S_d}{N_d} - \mu_d S_d \tag{1}$$

$$\frac{dE_d}{dt} = \frac{b_{fd}\beta_{fd}I_f S_d}{N_d} - \tau_d E_d - \mu_d E_d \tag{2}$$

$$\frac{dI_d}{dt} = \tau_d E_d - r_d I_d - d_d I_d - \mu_d I_d \tag{3}$$

$$\frac{dR_d}{dt} = r_d I_d - \mu_d R_d \tag{4}$$

where S_d denotes the number of susceptible dogs, E_d denotes the number of exposed/infected dogs, I_d denotes the number of infectious dogs, R_d denotes the number of recovered dogs, and N_d denotes the total number of dogs.

The above model is a classic SEIR model. In Eq. (1), a constant birth rate λ_d was used for susceptible dogs, the amount of $b_{fd}\beta_{fd}I_f S_d/N_d$ susceptible dogs were moved from compartment S_d (susceptible population) to E_d (exposed/infected population) due to ZVL transmission where S_d/N_d denotes the contact rate between

susceptible dogs and sand flies, and $\mu_d S_d$ susceptible dogs were removed because of natural death. Similarly, in Eq. (2) $\tau_d E_d$ exposed/infected dogs (from compartment E_d) became infectious dogs (into compartment I_d) and $\mu_d E_d$ exposed dogs were removed due to natural death. In Eq. (3), a portion of $r_d I_d$ infectious dogs recovered and converted to R_d, but $d_d I_d$ more infectious dogs died due to the disease or culling strategy, in addition to $\mu_d I_d$ natural deaths. Recovered dogs remained under treatment and were assumed to not be reinfected and $\mu_d R_d$ ones were removed because of natural death. In addition, E_d could be seropositive but not culled or dead due to the disease (This was assumed as these animals are, at least in theory, infected but not yet tested).

2.2 Sand fly population

$$\frac{dS_f}{dt} = \lambda_f - \frac{b_{fd}\beta_{df} I_d S_f}{N_d} - m_f S_f - \mu_f S_f \tag{5}$$

$$\frac{dE_f}{dt} = \frac{b_{fd}\beta_{df} I_d S_f}{N_d} - \tau_f E_f - m_f E_f - \mu_f E_f \tag{6}$$

$$\frac{dI_f}{dt} = \tau_f E_f - d_f I_f - m_f I_f - \mu_f I_f \tag{7}$$

where S_f denotes the number of susceptible sand flies, E_f denotes the number of exposed/infected sand flies, I_f denotes the number of infectious sand flies.

The above model is a SEI model similar to the system in Sect. 2.1 but without the recovered stage. With a constant birth rate λ_f for susceptible sand flies, $b_{fd}\beta_{df} I_d S_f / N_d$ susceptible sand flies moved from compartment S_f (susceptible) to E_f (exposed/infected) due to ZVL transmission via contacts between infectious dogs and susceptible sand flies, and $\mu_f S_f$ susceptible sand flies were eliminated because of natural death. The portion of $\tau_f E_f$ exposed sand flies became infectious sand flies, and $\mu_f E_f$ exposed sand flies are expired due to natural death. In Eq. (7), the portion of $d_f I_f$ more infectious sand flies expired due to the disease, in addition to $\mu_f I_f$ natural deaths. Infectious sand flies cannot recover from the disease. Moreover, $m_f(S_f + E_f + I_f)$ sand flies were assumed to emigrate from the system.

2.3 Human population

$$\frac{dS_h}{dt} = \lambda_h - \frac{b_{fh}\beta_{fh} I_f S_h}{N_h} - \mu_h S_h \tag{8}$$

$$\frac{dE_h}{dt} = \frac{b_{fh}\beta_{fh} I_f S_h}{N_h} - \tau_h E_h - \mu_h E_h \tag{9}$$

$$\frac{dI_h}{dt} = \tau_h E_h - \delta_h I_h - d_I I_h - r_I I_h - \mu_h I_h \tag{10}$$

$$\frac{dH_h}{dt} = \delta_h I_h - d_H H_h - r_H H_h - \mu_h H_h \tag{11}$$

$$\frac{dR_h}{dt} = r_H H_h + r_I I_h - \mu_h R_h \tag{12}$$

where S_h denotes the number of susceptible individuals, E_h denotes the number of exposed individuals, I_h denotes the number of infected individuals, H_h denotes the number of hospitalized individuals, and R_h denotes the number of recovered individuals, and N_h denotes the total number of humans.

The above model is a modified SEIR model with compartment H_h, which represents the number of individuals who are taken to the hospital by family and/or health authorities with regards to infected and symptomatic people. A constant birth rate λ_h exists for susceptible individuals. In Eq. (8), the amount of $b_{fh}\beta_{fh} I_f S_h / N_h$ susceptible individuals moved from compartment S_h to E_h due to ZVL transmission, and $\mu_h S_h$ susceptible individuals were removed because of natural death. For exposed individuals in Eq. (9), $\tau_h E_h$ became infected individuals, and $\mu_h E_h$ exposed individuals were removed due to natural death. In Eq. (10), $\delta_h I_h$ infected individuals are taken to the hospital and move to compartment H_h and $d_I I_h$ of them died due to the disease before they went to the hospital. We assume few infected individuals, $r_I I_h$, recovered and moved to recovered individuals. For hospitalized individuals in Eq. (11), $r_H H_h$ recovered and converted to recovered individuals and $d_H H_h$ expires because of disease. In Eq. (12), recovered individuals could not be reinfected so that only $\mu_h R_h$ are removed due to natural death.

2.4 Well-posedness of the solutions

Considering the physical meaning of ZVL transmissions, only nonnegative initial conditions are used and negative solutions are not allowed. All parameters in the system are nonnegative as well. In this section, we prove that all solutions in Eqs. (1)–(12) are nonnegative if initial conditions are nonnegative and they are bounded.

Proof According to Theorem 2.1 in (Smith 2008) which is

"Assume that whenever $\phi \in D$ satisfies $\phi \geq 0$, $\phi_i(0) = 0$ for some i and $t \in R$, then $f_i(t, \phi) \geq 0$. If $\phi \in D$ satisfies $\phi \geq 0$ and $t_0 \in R$, then $f_i(t, \phi) \geq 0$".

It is easy to test that all of our equations satisfy the conditions in the above theorem so that we know $S_d(t) \geq 0$, $E_d(t) \geq 0$, $I_d(t) \geq 0$, $R_d(t) \geq 0$, $S_f(t) \geq 0$, $E_f(t) \geq 0$, $I_f(t) \geq 0$, $S_h(t) \geq 0$, $E_h(t) \geq 0$, $I_h(t) \geq 0$, $H_h(t) \geq 0$, and $R_h(t) \geq 0$, if $S_d(0) \geq 0$, $E_d(0) \geq 0$, $I_d(t) \geq 0$, $R_d(t) \geq 0$, $S_f(t) \geq 0$, $E_f(t) \geq 0$, $I_f(t) \geq 0$, $S_h(t) \geq 0$, $E_h(t) \geq 0$, $I_h(t) \geq 0$, $H_h(t) \geq 0$, and $R_h(t) \geq 0$.

Based on Eqs. (1)–(12), we have

$$\frac{dN_d}{dt} = \lambda_d - d_d I_d - \mu_d N_d \tag{13}$$

$$\frac{dN_f}{dt} = \lambda_f - m_f N_f - d_f I_f - \mu_f N_f \tag{14}$$

$$\frac{dN_h}{dt} = \lambda_h - d_I I_h - d_H H_h - \mu_h N_h \tag{15}$$

where $N_d = S_d + E_d + I_d + R_d$, $N_f = S_f + E_f + I_f$, $N_h = S_h + E_h + I_h + H_h + R_h$. When $t \to \infty$, we have $N_d < \lambda_d/\mu_d$, $N_f < \lambda_f/(m_f + \mu_f)$, $N_h < \lambda_h/\mu_h$ since $d_d, I_d, d_f, I_f, d_I, I_h, d_H, H_h \geq 0$. Hence, N_d, N_f, and N_h are bounded. Then $S_d, E_d, I_d, R_d, S_f, E_f, I_f, S_h, E_h, I_h, H_h$, and R_h are bounded since they are all nonnegative.

2.5 Calculation of R_0

The basic ratio R_0 is defined as the average number of secondary cases arising from an average primary case in an entirely susceptible population (Keeling and Rohani 2008). This ratio can be solved based on disease free equilibrium (DFE).

The entire system [Eqs. (1)–(12)] has a DFE given by

$$\begin{aligned} E_0 &= (S_d^*, E_d^*, I_d^*, R_d^*, S_f^*, E_f^*, I_f^*, S_h^*, E_h^*, I_h^*, H_h^*, R_h^*) \\ &= \left(\frac{\lambda_d}{\mu_d}, 0, 0, 0, \frac{\lambda_f}{\mu_f + m_f}, 0, 0, \frac{\lambda_h}{\mu_h}, 0, 0, 0, 0\right) \end{aligned} \tag{16}$$

Linear stability of E_0 can be established using the next generation operator method (Garba et al. 2008). Matrices $\mathbf{F}$ (for the rate of appearance of new infections) and $\mathbf{V}$ (for the rate of transfer of individuals) are given, respectively, by:

$$\mathbf{F} = \begin{bmatrix} 0 & 0 & 0 & 0 & \frac{b_{fd}\beta_{fd}S_d^*}{N_d^*} & 0 & 0 & 0 & 0 \\ 0 & 0 & 0 & 0 & 0 & 0 & 0 & 0 & 0 \\ 0 & 0 & 0 & 0 & 0 & 0 & 0 & 0 & 0 \\ 0 & \frac{b_{fd}\beta_{df}S_f^*}{N_d^*} & 0 & 0 & 0 & 0 & 0 & 0 & 0 \\ 0 & 0 & 0 & 0 & 0 & 0 & 0 & 0 & 0 \\ 0 & 0 & 0 & 0 & \frac{b_{fh}\beta_{fh}S_h^*}{N_h^*} & 0 & 0 & 0 & 0 \\ 0 & 0 & 0 & 0 & 0 & 0 & 0 & 0 & 0 \\ 0 & 0 & 0 & 0 & 0 & 0 & 0 & 0 & 0 \\ 0 & 0 & 0 & 0 & 0 & 0 & 0 & 0 & 0 \end{bmatrix} \tag{17}$$

$$\mathbf{V} = \begin{bmatrix} k_1 & 0 & 0 & 0 & 0 & 0 & 0 & 0 & 0 \\ \tau_d & k_2 & 0 & 0 & 0 & 0 & 0 & 0 & 0 \\ 0 & -r_d & \mu_d & 0 & 0 & 0 & 0 & 0 & 0 \\ 0 & 0 & 0 & k_4 & 0 & 0 & 0 & 0 & 0 \\ 0 & 0 & 0 & -\tau_f & k_5 & 0 & 0 & 0 & 0 \\ 0 & 0 & 0 & 0 & 0 & k_6 & 0 & 0 & 0 \\ 0 & 0 & 0 & 0 & 0 & -\tau_h & k_7 & 0 & 0 \\ 0 & 0 & 0 & 0 & 0 & 0 & -\delta_h & k_8 & 0 \\ 0 & 0 & 0 & 0 & 0 & 0 & -r_I & -r_H & \mu_h \end{bmatrix} \tag{18}$$

where $k_1 = \tau_d + \mu_d$, $k_2 = r_d + d_d + \mu_d$, $k_4 = \tau_f + m_f + \mu_f$, $k_5 = d_f + m_f + \mu_f$, $k_6 = \tau_h + \mu_h$, $k_7 = \delta_h + d_I + r_I + \mu_h$, $k_8 = d_H + r_H + \mu_h$, $N_d^* = S_d^*$, and $N_h^* = S_h^*$.

Therefore, the basic reproduction number, denoted by R_0, is given by

$$R_0 = \rho(\mathbf{FV}^{-1}) = \frac{b_{fd}\sqrt{k_1 k_2 k_4 k_5 \beta_{fd}\beta_{df}\tau_d\tau_f S_d^* S_f^*}}{k_1 k_2 k_4 k_5 N_d^*} \tag{19}$$

where ρ is the spectral radius (dominant eigenvalue in magnitude or maximum of the absolute values of eigenvalues of the matrix).The threshold quantity R_0, the basic reproduction number of the disease, represents the average number of secondary cases that one infected case can generate if introduced into a completely susceptible population. Hence, using Theorem 2 of (Garba et al. 2008), we established the following result: disease free equilibrium, E_0, of the system [Eqs. (1)–(12)], is locally asymptotically stable (LAS) if $R_0 < 1$ and unstable if $R_0 > 1$.

In general, when R_0 is less than unity, a small influx of infected sand flies into the community does not generate large outbreaks, and the disease dies out in the end (since DFE is LAS). However, as we demonstrate in Sect. 3, the disease may persist even when $R_0 < 1$.

3 Backward bifurcation

3.1 Backward bifurcation

In Castillo-Chavez and Song (2004), the conjecture was made that the zoonotic disease model may exhibit backward bifurcation. In order to find endemic equilibria of the system in Sect. 2 (equilibrium in which at least one of the infected components is non-zero), the following steps was taken.

$E_1 = (S_d^{**}, E_d^{**}, I_d^{**}, R_d^{**}, S_f^{**}, E_f^{**}, I_f^{**}, S_h^{**}, E_h^{**}, I_h^{**}, H_h^{**}, R_h^{**})$ represents any arbitrary endemic equilibrium of the model. Let $\theta_d^{**} = \frac{b_{fd}\beta_{fd}I_f^{**}}{N_d^{**}}$, $\theta_f^{**} = \frac{b_{fd}\beta_{df}I_d^{**}}{N_d^{**}}$, $\theta_h^{**} = \frac{b_{fh}\beta_{fh}I_f^{**}}{N_h^{**}}$, where $N_d^{**} = S_d^{**} + E_d^{**} + I_d^{**} + R_d^{**}$, $N_h^{**} = S_h^{**} + E_h^{**} + I_h^{**} + H_h^{**} + R_h^{**}$.

Solving the equations at steady state gives

$$S_d^{**} = \frac{\lambda_d}{\theta_d^{**} + \mu_d} \tag{20}$$

$$E_d^{**} = \frac{\theta_d^{**}\lambda_d}{k_1(\theta_d^{**} + \mu_d)} \tag{21}$$

$$I_d^{**} = \frac{\theta_d^{**}\tau_d\lambda_d}{k_1 k_2(\theta_d^{**} + \mu_d)} \tag{22}$$

$$R_d^{**} = \frac{\theta_d^{**}\tau_d\lambda_d r_d}{k_1 k_2\mu_d(\theta_d^{**} + \mu_d)} \tag{23}$$

$$S_f^{**} = \frac{\lambda_f}{\theta_f^{**} + k_3} \tag{24}$$

$$E_f^{**} = \frac{\theta_f^{**}\lambda_f}{k_4(\theta_f^{**} + k_3)} \tag{25}$$

$$I_f^{**} = \frac{\theta_f^{**}\lambda_f\tau_f}{k_4k_5(\theta_f^{**} + k_3)} \tag{26}$$

$$S_h^{**} = \frac{\lambda_h}{\theta_h^{**} + \mu_h} \tag{27}$$

$$E_h^{**} = \frac{\theta_h^{**}\lambda_h}{k_6(\theta_h^{**} + \mu_h)} \tag{28}$$

$$I_h^{**} = \frac{\theta_h^{**}\lambda_h\tau_h}{k_6k_7(\theta_h^{**} + \mu_h)} \tag{29}$$

$$H_h^{**} = \frac{\theta_h^{**}\lambda_h\tau_h\delta_h}{k_6k_7k_8(\theta_h^{**} + \mu_h)} \tag{30}$$

$$R_h^{**} = \frac{\theta_h^{**}\lambda_h\tau_h(\delta_h r_H + r_I k_8)}{k_6k_7k_8\mu_h(\theta_h^{**} + \mu_h)} \tag{31}$$

Substituting Eqs. (20)–(31) in θ_d^{**} and θ_f^{**} and simplifying after algebraic manipulations respectively gives

$$\theta_d^{**} = \frac{b_{fd}\beta_{fd}\tau_f\lambda_f k_1k_2\mu_d\theta_f^{**}(\theta_d^{**} + \mu_d)}{(\theta_f^{**} + k_3)k_4k_5[k_2\mu_d\lambda_d\left(k_1 + \theta_d^{**}\right) + \tau_d\lambda_d\theta_d^{**}(\mu_d + r_d)]} \tag{32}$$

$$\theta_f^{**} = \frac{b_{fd}\beta_{df}\tau_d\mu_d\theta_d^{**}}{k_2\mu_d\left(k_1 + \theta_d^{**}\right) + \tau_d\theta_d^{**}(\mu_d + r_d)} \tag{33}$$

Substitution of (33) in (32) shows that non-zero equilibria of the model satisfies the following quadratic (in terms of θ_d^{**})

$$a_0\left(\theta_d^{**}\right)^2 + b_0(\theta_d^{**}) + c_0 = 0 \tag{34}$$

where $a_0 = k_4k_5\lambda_d[k_2b_{fd}\beta_{df}\tau_d\mu_d^2 + k_2^2k_3\mu_d^2 + b_{fd}\beta_{df}\tau_d^2\mu_d(\mu_d + r_d) + 2k_2k_3\mu_d\tau_d(\mu_d + r_d) + k_3\tau_d^2(\mu_d + r_d)^2]$, $b_0 = k_1k_2k_4k_5\mu_d\lambda_d[b_{fd}\beta_{df}\tau_d\mu_d + 2k_2k_3\mu_d + 2k_3\tau_d(\mu_d + r_d) - k_1k_2k_3R_0^2]$, $c_0 = k_1^2k_2^2k_3k_4k_5\mu_d^2\lambda_d(1 - R_0^2)$.

The quadratic equation can be analyzed for the possibility of multiple endemic equilibriums (Blayneh et al. 2010). We achieved positive equilibrium of the system by solving for θ_d^{**} from the quadratic equation (34) and substituting the results (positive value of θ_d^{**}) into expressions in Eqs. (20)–(31). From above formula, the coefficient a_0 of (34) is always positive and c_0 is positive (negative) if R_0 is less than (greater than) one, respectively. Therefore, the following result is established:

Theorem 1 *The system has:*

(i) *A unique endemic equilibrium exist if* $c_0 < 0$*;*
(ii) *A unique endemic equilibrium exist if* $b_0 < 0$*,and* $c_0 = 0$ *or* $b_0^2 - 4a_0c_0 = 0$*;*
(iii) *Two endemic equilibriums exist if* $c_0 > 0$, $b_0 < 0$ *and* $b_0^2 - 4a_0c_0 > 0$*;*
(iv) *No endemic equilibrium exist otherwise.*

This method, also used in a Dengue model (Garba et al. 2008), is a general way to evaluate the system. Theorem 1 (Case i) clearly demonstrates that the model has a unique endemic equilibrium when $R_0 > 1$. Case (iii) indicates the possibility of backward bifurcation in which local asymptotically stable DFE co-exists with a locally-asymptotically stable endemic equilibrium when $R_0 < 1$. In this case, we possibly reach an endemic equilibrium instead of DFE even when $R_0 < 1$, depending on how many infections occur in the population at the beginning. A critical value of R_0, denoted by R_c, is given by setting $b_0^2 - 4a_0c_0 = 0$. Considering the physical meaning of each parameter, we could numerically test that only one solution of R_c is possible among four roots of the equation. To simplify the notation, let $b_1 = k_1k_2k_4k_5\mu_d\lambda_d$, $b_2 = b_{fd}\beta_{df}\tau_d\mu_d + 2k_2k_3\mu_d + 2k_3\tau_d(\mu_d + r_d)$, $b_3 = k_1k_2k_3$, $c_1 = k_1^2k_2^2k_3k_4k_5\mu_d^2\lambda_d$, we have:

$$R_c = \sqrt[2]{\frac{-B_0 + \sqrt[2]{B_0^2 - 4A_0C_0}}{2A_0}} \tag{35}$$

where $A_0 = b_1^2b_3^2$, $B_0 = 4a_0c_1 - 2b_1^2b_2b_3$, $C_0 = b_1^2b_2^2 - 4a_0c_1$.

R_c is critical because no endemics equilibrium exists when $R_0 < R_c$. To successfully control the spread of ZVL, the reproduction number should be brought below R_c. Condition $R_0 < 1$ is not sufficient for a complete control of the spread of ZVL described; therefore, backward bifurcation would occur for values of R_0 such that $R_c < R_0 < 1$.

Before analyzing the conditions of backward bifurcation, we presented numerical solutions for a given range of each parameter using Mathematica. For example, we simulated the model with a set of parameters that satisfies the condition of Case (iii) which also satisfies the reasonable range for each parameter. The values applied are $\lambda_d = 25, \lambda_f = 65, \lambda_h = 25, \mu_d = 0.0014, \mu_f = 0.022, \mu_h = 8.3e-5, b_{fd} = 0.1, b_{fh}$=0.1, $\beta_{fd} = 0.5, \beta_{df} = 0.7, \beta_{fh} = 0.5, d_d = 0.017, d_f = 0, d_I = 0.0067, d_H = 0.0003, m_f = 0.0001, \tau_d = 0.1, \tau_f = 0.167, \tau_h = 0.0167, \delta_h = 0.8, r_d = 0.005, r_I = 0.12$, and $r_H = 0.95$ (Stauch et al. 2011; Blayneh et al. 2010). With this set of parameters, $R_c = 0.968 < 1$ and $R_0 = 0.985 < 1$ (so that, $R_c < R_0 < 1$). The infectious dog population versus R_0 with the associated bifurcation diagram is depicted in Fig. 2. In Region A, disease free equilibrium is locally asymptotically stable which indicates that the disease cannot spread out and the status would change back to disease free equilibrium if we have a few infected individuals in the beginning, while in Region B, one disease-persistent equilibrium is stable (little perturbation could not change the equilibrium status) and the other is unstable (little perturbation could change the status of the system and change to another equilibrium status, i.e. disease free equilibrium), thereby showing the coexistence of two stable

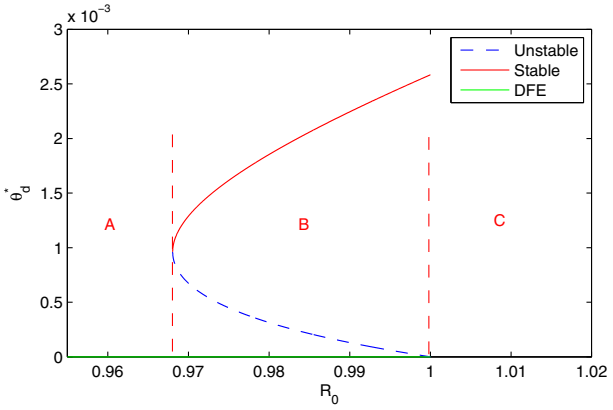

Fig. 2 Bifurcation diagram of the system

Table 2 Summary of backward bifurcation shown in Fig. 2

Region	R_0	Type of steady states	Stability of steady state
A	<0.968	DFE	Stable
B	0.968−1	A DFE and two endemic equilibria	The DFE and one endemic equilibrium are stable while the other endemic equilibrium is unstable
C	>1	A DFE and one endemic equilibrium	The DFE is unstable while the endemic equilibrium is stable

equilibria when $R_c < R_0 < 1$ and confirming that the system exhibits backward bifurcation. Disease-persistent equilibrium is stable in Region C. Results shown in Fig. 2 are summarized in Table 2.

To analyze the relationship between R_c and all possible parameters involved, we decide to focus on the parameters that are likely amenable to control and possibly represent the reality in the field (dogs, sand flies, and humans). In optimal control section, reduction of infection rate to dogs and humans, and use of insecticide against sand flies are considered. Hence, β_{fd}, β_{fh}, and μ_f are studied in order to figure out their impacts on R_0 and R_c.

The value of R_c is not dependent on the parameter β_{fd} while the value of R_0 increases as β_{fd} increases. And therefore, we could find a range (shown in Fig. 3a) which satisfies the condition $R_C < R_0 < 1$ if we could change the infection rate to dogs.

It is surprising that neither of R_0 and R_c are dependent on the parameter β_{fh}, implying that the infection rate to humans does not affect the value of R_0 and R_c. Hence, humans do not contribute to the spread of disease since dogs and sand flies are not infected by humans. Although controlling the infection rate to humans will

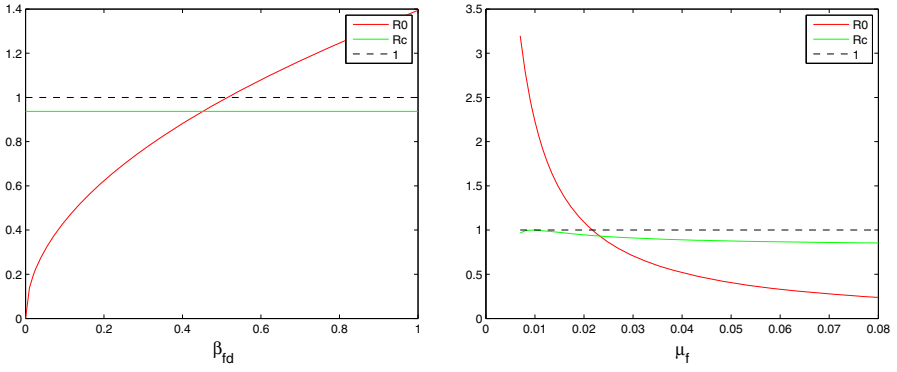

Fig. 3 Impacts of parameters on backward bifurcation

not impact the stability of disease free equilibrium, it is still very important when we discuss the optimal control strategies since reduction of the number of infected humans is one of our objectives. The optimal control strategies will be discussed in the next section.

For the last parameter μ_f, it can affect the values of both of R_0 and R_c. The relationship between R_0 and μ_f and between R_c and μ_f is shown in Fig. 3b. There is only a narrow range which satisfies the condition $R_C < R_0 < 1$. However, the value of R_0 is very sensitive to the value of μ_f, which shows that use of insecticide against sand flies is a good strategy if the insecticide is effective towards increasing the mortality rate of sand files.

A more general simulation is modeled using Mathematica which allow us to adjust the values of several model parameters and observe the simulation results in a dynamic fashion. Figure 4 shows a screenshot of this dynamical model which illustrates backward bifurcation for ZVL. I_d^{**} represents the number of infectious dogs at the endemic equilibrium point. The green curve represents a stable endemic equilibrium and the red dot curve represents an unstable endemic equilibrium. The intersection between two curves is a critical threshold R_c for backward bifurcation (which is represented using a red line in Fig. 4). When $R_0 < R_c$, we only have one disease free equilibrium. When $R_c < R_0 < 1$, we have three equilibria: one stable disease free equilibrium, one unstable endemic equilibrium, and one stable endemic equilibrium. It turns out that if we have an endemic equilibrium in which the number of infectious dogs is in the range of the green line, we cannot control the spread of ZVL even if $R_0 < 1$. In the Fig. 2, R_0 is calculated in terms of given parameters and it is in the range between R_c and 1. In this case, it is possible that we cannot control the spread of ZVL if we already have a certain number of infectious dogs.

Analysis and simulation result established the following result: the model constructed in Sect. 2 underwent backward bifurcation when Case (iii) of Theorem 1 holds and $R_c < R_0 < 1$.

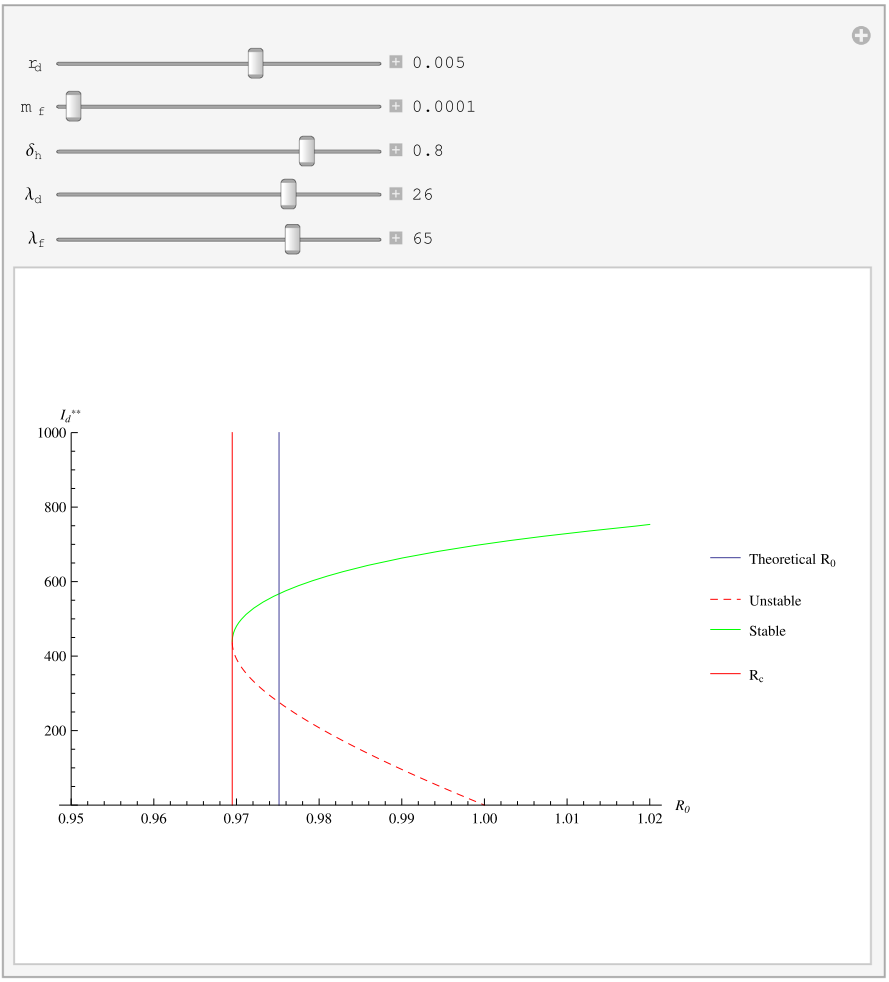

Fig. 4 General simulation with various parameter values

3.2 Stability of the endemic equilibrium

To discuss the stability of the endemic equilibrium, we need to determine the eigenvalues of the Jacobian matrix evaluated at the endemic equilibrium (Zhang et al. 2014b, a). Considering the complexity of the system, the calculation of eigenvalues is meaningful. However, we are interested in the stability of endemic equilibrium around $R_0 = 1$. And therefore, the centre manifold theory is considered.

Let $\phi = \beta_{fd}$ as the bifurcation parameter, when $R_0 = 1$, we have $\phi = \frac{k_1 k_2 k_4 k_5 \lambda_d (\mu_f + m_f)}{\mu_d \lambda_f b_{fd}^2 \beta_{df} \tau_d \tau_f}$.

The Jacobian matrix of the dogs-sand flies-humans system at DFE when $\phi = \beta_{fd}$, is given below:

$$\mathbf{J}=\begin{bmatrix}
-\mu_d & 0 & 0 & 0 & 0 & -b_{fd}\phi & 0 & 0 & 0 & 0 & 0 & 0\\
0 & -k_1 & 0 & 0 & 0 & b_{fd}\phi & 0 & 0 & 0 & 0 & 0 & 0\\
0 & \tau_d & -k_2 & 0 & 0 & 0 & 0 & 0 & 0 & 0 & 0 & 0\\
0 & 0 & r_d & -\mu_d & 0 & 0 & 0 & 0 & 0 & 0 & 0 & 0\\
0 & 0 & -\frac{b_{fd}\beta_{df}S_f^*}{N_d^*} & 0 & -k_3 & 0 & 0 & 0 & 0 & 0 & 0 & 0\\
0 & 0 & \frac{b_{fd}\beta_{df}S_f^*}{N_d^*} & 0 & 0 & -k_4 & 0 & 0 & 0 & 0 & 0 & 0\\
0 & 0 & 0 & 0 & 0 & \tau_f & -k_5 & 0 & 0 & 0 & 0 & 0\\
0 & 0 & 0 & 0 & 0 & 0 & -b_{fh}\beta_{fh} & -\mu_h & 0 & 0 & 0 & 0\\
0 & 0 & 0 & 0 & 0 & 0 & b_{fh}\beta_{fh} & 0 & -k_6 & 0 & 0 & 0\\
0 & 0 & 0 & 0 & 0 & 0 & 0 & 0 & \tau_h & -k_7 & 0 & 0\\
0 & 0 & 0 & 0 & 0 & 0 & 0 & 0 & 0 & \delta_h & -k_8 & 0\\
0 & 0 & 0 & 0 & 0 & 0 & 0 & 0 & 0 & r_I & r_H & -\mu_h
\end{bmatrix} \tag{36}$$

We use Mathematica to calculate the eigenvalue of the Jacobian $J(\phi)$ and note that there is a simple zero eigenvalue. Hence, the centre manifold theory can be used to analyze the dynamics of the dogs-sand flies-humans system.

Let $w = (w_1, w_2, w_3, w_4, w_5, w_6, w_7, w_8, w_9, w_{10}, w_{11}, w_{12})^T$ be the right eigenvector associated with zero eigenvalue, we have

$$w_1 = -\frac{\lambda_d k_1 k_2 k_3 k_4 w_6}{\beta_{df} b_{fd} \lambda_f \mu_d^2 \tau_d} \tag{37}$$

$$w_2 = \frac{\lambda_d k_2 k_3 k_4 w_6}{\beta_{df} b_{fd} \lambda_f \mu_d \tau_d} \tag{38}$$

$$w_3 = \frac{\lambda_d k_3 k_4 w_6}{\beta_{df} b_{fd} \lambda_f \mu_d} \tag{39}$$

$$w_4 = \frac{\lambda_d r_d k_3 k_4 w_6}{\beta_{df} b_{fd} \lambda_f \mu_d^2} \tag{40}$$

$$w_5 = -\frac{k_4 w_6}{k_3} \tag{41}$$

$$w_6 = w_6 \tag{42}$$

$$w_7 = \frac{\tau_f w_6}{k_5} \tag{43}$$

$$w_8 = -\frac{\beta_{fh} b_{fh} \tau_f w_6}{k_5 \mu_h} \tag{44}$$

$$w_9 = \frac{\beta_{fh} b_{fh} \tau_f w_6}{k_5 k_6} \tag{45}$$

$$w_{10} = \frac{\beta_{fh} b_{fh} \tau_f \tau_h w_6}{k_5 k_6 k_7} \tag{46}$$

$$w_{11} = \frac{\beta_{fh} b_{fh} \delta_h \tau_f \tau_h w_6}{k_5 k_6 k_7 k_8} \tag{47}$$

$$w_{12} = \frac{\beta_{fh} b_{fh} (\delta_h r_H + d_H r_I + \mu_h r_I + r_H r_I) \tau_f \tau_h w_6}{\mu_h k_5 k_6 k_7 k_8} \tag{48}$$

Similarly, the corresponding left eigenvector $v = (v_1, v_2, v_3, v_4, v_5, v_6, v_7, v_8, v_9, v_{10}, v_{11}, v_{12})^T$, where $v_1 = 0, v_2 = v_2, v_3 = \frac{k_1 v_2}{\tau_d}, v_4 = v_5 = 0, v_6 = \frac{\lambda_d k_1 k_2 k_3 v_2}{\beta_{df} b_{fd} \lambda_f \mu_d \tau_d}, v_7 = \frac{\lambda_d k_1 k_2 k_3 k_4 v_2}{\beta_{df} b_{fd} \lambda_f \mu_d \tau_d \tau_f}, v_8 = v_9 = v_{10} = v_{11} = v_{12} = 0$.

To simplify the notation, let $S_d = x_1$, $E_d = x_2$, $I_d = x_3$, $R_d = x_4$, $S_f = x_5$, $E_f = x_6$, $I_f = x_7$, $S_h = x_8$, $E_h = x_9$, $I_h = x_{10}$, $H_h = x_{11}$, and $R_h = x_{12}$. In addition, assume $\frac{dS_d}{dt} = f_1$, $\frac{dE_d}{dt} = f_2$, $\frac{dI_d}{dt} = f_3$, $\frac{dR_d}{dt} = f_4$, $\frac{dS_f}{dt} = f_5$, $\frac{dE_f}{dt} = f_6$, $\frac{dI_f}{dt} = f_7$, $\frac{dS_h}{dt} = f_8$, $\frac{dE_h}{dt} = f_9$, $\frac{dI_h}{dt} = f_{10}$, $\frac{dH_h}{dt} = f_{11}$, $\frac{dR_h}{dt} = f_{12}$.

Let

$$a = \frac{1}{2} \sum_{i,j,k=1}^{n} v_i w_j w_k \frac{\partial^2 f_i}{\partial x_j \partial x_k}(E_0, 0) \tag{49}$$

$$b = \sum_{i,j=1}^{n} v_i w_j \frac{\partial^2 f_i}{\partial x_j \partial \beta_{fd}}(E_0, 0) \tag{50}$$

If $b \neq 0$, the value of a (either positive or negative) determines the nature of the endemic equilibria near the $R_0 = 1$. In our system, we know $v_1 = v_4 = v_5 = v_8 = v_9 = v_{10} = v_{11} = v_{12} = 0$, so we only need to consider v_2, v_3, v_6, and v_7. In addition, the second derivative of f_3, and f_7 are equal to 0, so

$$a = \frac{1}{2} \left(v_2 \sum_{j,k=1}^{n} w_j w_k \frac{\partial^2 f_2}{\partial x_j \partial x_k}(E_0, 0) + v_6 \sum_{j,k=1}^{n} w_j w_k \frac{\partial^2 f_6}{\partial x_j \partial x_k}(E_0, 0) \right) \tag{51}$$

$$b = v_2 \sum_{j=1}^{n} w_j \frac{\partial^2 f_2}{\partial x_j \partial \beta_{fd}}(E_0, 0) \tag{52}$$

Solve a and b, we have $a = -m_{11}\phi + m_{22}$, $b = v_2 w_7 b_{fd} \neq 0$, where

$$m_{11} = v_2 w_7 (w_2 + w_3 + w_4) b_{fd} \mu_d / \lambda_d \tag{53}$$

$$m_{22} = \frac{v_6 w_3 b_{fd} \beta_{df} \mu_d}{\lambda_d} \left(w_5 - \frac{\lambda_f \mu_d w_1 w_2 w_3 w_4}{\lambda_d (\mu_f + m_f)} \right) \tag{54}$$

Based on the theorem in (Van den Driessche and Watmough 2002), if $\phi > \frac{m_{22}}{m_{11}}$, then $a < 0$ and the system undergoes a forward bifurcation and there are locally asymptotically stable endemic equilibria near DFE for $R_0 > 1$; while if $\phi < \frac{m_{22}}{m_{11}}$, the system has a backward bifurcation and there are unstable endemic equilibrium near DFE for $R_0 < 1$.

The epidemiological significance of backward bifurcation is that the classical requirement of $R_0 < 1$, although necessary, is no longer sufficient for disease elimination. In such a scenario, disease elimination depends on initial sizes of sub-populations (state variables) of the model. In other words, backward bifurcation in the ZVL transmission model suggests feasibility of controlling ZVL when $R_0 < 1$ could be

dependent on initial sizes of the sub-population of the model. Therefore, methods for disease control must be improved.

4 Optimal control

In this section, we extend the model in Sect. 2 to include density-dependent mortality rates in sand fly populations and recruitment rate in each susceptible population.

Define the density-dependent mortality rate for sand flies $\mu_f = \mu_1 + \mu_2 N_f$, where μ_1 is the density-independent death rate in the sand fly population, μ_2 is proportionality constant and N_f is the total number of sand flies. Similarly, we replaced previous recruitment rates to density-dependent recruitment rate by $\lambda_d \to \lambda_d + \rho N_d$, $\lambda_f \to \lambda_f N_f$, and $\lambda_h \to \lambda_h + \gamma_h N_h$, where ρ and γ_h are proportionality constants showing the impact of density on recruitment rates.

Three time-dependent control strategies, $u_1(t)$, $u_2(t)$, and $u_3(t)$, regarding populations of dogs, sand flies, and human, respectively, are described in this section.

In the dog population, the associated force of infection was reduced by a factor of $(1 - u_1(t))$, where $u_1(t)$ measures the level of successful prevention measures (vaccine protection). From the literature review, canine leishmaniasis (known as CanV or CanVL) was considered one of a few parasitic diseases likely to be controllable by vaccination (Ramiro et al. 2003; Kedzierski et al. 2006). The strategy of culling dogs carries ethic and humanitarian issues, and it is not included as part of the three time-dependent control strategies in our studies but the model can easily address this issue by varying parameter d_d in the model [i.e., Eq. (3) in Sect. 2.1].

In the sand fly population, control strategy $u_2(t)$ represented the level of insecticide used for sand fly control administered at sand fly breeding sites. Consequently, the reproduction rate of the sand fly population was reduced by a factor of $(1-u_2(t))$. The assumption was made that the mortality rate of sand fly increases at a rate proportional to $u_2(t)$, where $r_0 > 0$ is a rate constant.

In the human population, the associated force of infection was reduced by a factor of $(1-u_3(t))$, where $u_3(t)$ measures the level of successful prevention (personal protection) efforts. Therefore, $u_3(t)$ indicates the use of alternative preventive measures to minimize or eliminate sand fly-human contacts.

Accounting for the above assumptions and extensions, the extended ZVL model with control strategy terms was constructed:

$$\frac{dS_d}{dt} = \lambda_d + \rho N_d - \frac{b_{fd}\beta_{fd} I_f S_d (1-u_1(t))}{N_d} - \mu_d S_d \tag{55}$$

$$\frac{dE_d}{dt} = \frac{b_{fd}\beta_{fd} I_f S_d (1-u_1(t))}{N_d} - \tau_d E_d - \mu_d E_d \tag{56}$$

$$\frac{dI_d}{dt} = \tau_d E_d - r_d I_d - d_d I_d - \mu_d I_d \tag{57}$$

$$\frac{dR_d}{dt} = r_d I_d - \mu_d R_d \tag{58}$$

$$\frac{dS_f}{dt} = \lambda_f N_f (1-u_2(t)) - \frac{b_{fd}\beta_{df} I_d S_f}{N_d} - (m_f + \mu_1 + \mu_2 N_f + r_0 u_2(t)) S_f \tag{59}$$

$$\frac{dE_f}{dt} = \frac{b_{fd}\beta_{df} I_d S_f}{N_d} - \tau_f E_f - m_f E_f - (\mu_1 + \mu_2 N_f)E_f - r_0 u_2(t) E_f \quad (60)$$

$$\frac{dI_f}{dt} = \tau_f E_f - d_f I_f - m_f I_f - (\mu_1 + \mu_2 N_f) I_f - r_0 u_2(t) I_f \quad (61)$$

$$\frac{dS_h}{dt} = \lambda_h + \gamma_h N_h - \frac{b_{fh}\beta_{fh} I_f S_h (1 - u_3(t))}{N_h} - \mu_h S_h \quad (62)$$

$$\frac{dE_h}{dt} = \frac{b_{fh}\beta_{fh} I_f S_h (1 - u_3(t))}{N_h} - \tau_h E_h - \mu_h E_h \quad (63)$$

$$\frac{dI_h}{dt} = \tau_h E_h - \delta_h I_h - d_I I_h - r_I I_h - \mu_h I_h \quad (64)$$

$$\frac{dH_h}{dt} = \delta_h I_h - d_H H_h - r_H H_h - \mu_h H_h \quad (65)$$

$$\frac{dR_h}{dt} = r_H H_h + r_I I_h - \mu_h R_h \quad (66)$$

Moreover, the rate of change of the total populations of dogs, sand flies, and humans is respectively given by

$$\frac{dN_d}{dt} = \lambda_d + \rho N_d - d_d I_d - \mu_d N_d \quad (67)$$

$$\frac{dN_f}{dt} = N_f[\lambda_f (1 - u_2(t)) - m_f - (\mu_1 + \mu_2 N_f) - r_0 u_2(t)] - d_f I_f \quad (68)$$

$$\frac{dN_h}{dt} = \lambda_h + \gamma_h N_h - d_I I_h - d_H H_h - \mu_h N_h \quad (69)$$

According to the extended model above, an optimal control problem with the objective function is formulated by

$$\text{Minimize } J(u_1, u_2, u_3) = \int_0^T (A_1 E_h(t) + A_2 I_h(t) + A_3 N_f(t) + B_1 u_1^2(t) + B_2 u_2^2(t) + B_3 u_3^2(t))dt \quad (70)$$

The objective is to minimize exposed and infected human populations, the total number of sand flies, and the cost of implementing the strategy. In Eq. (70), A_1, A_2, and A_3 represent weight constants of the exposed, infected human and the total number of sand flies. In addition, B_1, B_2, and B_3 are weight constants for dogs' prevention from disease, sand flies control, and human protection, respectively and $B_1 u_1^2(t)$, $B_2 u_2^2(t)$, and $B_3 u_3^2(t)$ describe the costs associated with dogs prevention, sand flies control, and human protection, respectively. These costs result from various sources. For example, cost associated with the first strategy primarily originates from the use of vaccination, cost associated with the second strategy primarily originates from the insecticide application, and cost associated with the third strategy originates from public health education to human populations, and testing equipment investments. We assumed that the costs are proportional to the square of the corresponding control function. Our goal was to determine optimal control functions (u_1^*, u_2^*, u_3^*) such that

$$J(u_1^*, u_2^*, u_3^*) = min(J(u_1, u_2, u_3)|(u_1, u_2, u_3) \in \Gamma) \tag{71}$$

Subject to the extended system, where $\Gamma = \{(u_1, u_2, u_3)|u_i(t)$ is Lebesgue measurable on $[0, T], 0 \leq u_i(t) \leq 1, i = 1, 2, 3\}$ is the control strategy set. The existence of an optimal control for the extended system would be proved and the optimality system would be derived.

4.1 Existence of an optimal control

Theorem 2 *Consider the objective function J given by Eq. (70) with* $(u_1, u_2, u_3) \in \Gamma$ *subject to the constraint state system [Eqs. (55)–(66)]. There exists* $(u_1^*, u_2^*, u_3^*) \in \Gamma$ *such that* $J(u_1^*, u_2^*, u_3^*) = min(J(u_1, u_2, u_3)|(u_1, u_2, u_3) \in \Gamma)$.

Proof The integrand of the objective function given by Eq. (70), $A_1E_h(t) + A_2I_h(t) + A_3N_f(t) + B_1u_1^2(t) + B_2u_2^2(t) + B_3u_3^2(t)$ is convex in the control strategy set Γ which is also convex and closed by definition. Conditions for the existence of optimal control are satisfied because the model is linear in the control variables and bounded by a linear system in the state variables (Fleming and Rishel 1975).

4.2 Optimality system

Pontryagins maximum principle (Pontryagin 1987) can be used for necessary conditions for an optimal control problem; the principle converts the problem into a problem of maximizing Hamilton H, with respect to u_1, u_2, u_3:

$$H = A_1E_h(t) + A_2I_h(t) + A_3N_f(t) + B_1u_1^2 + B_2u_2^2 + B_3u_3^2 + \sum_{i=1}^{12} \lambda_i f_i \tag{72}$$

where f_i is the right-hand side of the differential equation of i-th state variable. Application of Pontryagins Maximum Principle and the optimal control theory from (Fleming and Rishel 1975) achieved the following theorem:

Theorem 3 *Given an optimal control* $u^* = (u_1^*, u_2^*, u_3^*)$ *and corresponding state solutions* $S_d, E_d, I_d, R_d, S_f, E_f, I_f, S_h, E_h, I_h, H_h$, *and* R_h *of the corresponding state system, there adjoint functions,* λ_i, *exist for* $i = 1, 2, \ldots, 12$, *satisfying*

$$\lambda_1' = \frac{-\beta_{df}b_{fd}I_d\lambda_5S_f}{N_d^2} + \frac{\beta_{df}b_{fd}I_d\lambda_6S_f}{N_d^2} - \lambda_1\left(-\mu_d + \rho + \frac{\beta_{fd}b_{fd}I_fS_d(1-u_1)}{N_d^2} - \frac{\beta_{fd}b_{fd}I_f(1-u_1)}{N_d}\right) - \lambda_2\left(\frac{\beta_{fd}b_{fd}I_fS_d(1-u_1)}{N_d^2} + \frac{\beta_{fd}b_{fd}I_f(1-u_1)}{N_d}\right) \tag{73}$$

$$\lambda_2' = \frac{-\beta_{df}b_{fd}I_d\lambda_5S_f}{N_d^2} + \frac{\beta_{df}b_{fd}I_d\lambda_6S_f}{N_d^2} - \lambda_1\left(\rho + \frac{\beta_{fd}b_{fd}I_fS_d(1-u_1)}{N_d^2}\right)$$

$$-\lambda_2\left(-\mu_d-\tau_d-\frac{\beta_{fd}b_{fd}I_fS_d(1-u_1)}{N_d^2}\right)-\lambda_3\tau_d \tag{74}$$

$$\begin{aligned}\lambda_3^{'}=&-\lambda_3(-d_d-\mu_d-r_d)-\lambda_4r_d-\lambda_5\left(\frac{\beta_{df}b_{fd}I_dS_f}{N_d^2}-\frac{\beta_{df}b_{fd}S_f}{N_d}\right)\\&-\lambda_6\left(-\frac{\beta_{df}b_{fd}I_dS_f}{N_d^2}+\frac{\beta_{df}b_{fd}S_f}{N_d}\right)-\lambda_1\left(\rho+\frac{\beta_{fd}b_{fd}I_fS_d(1-u_1)}{N_d^2}\right)\\&+\lambda_2\frac{\beta_{fd}b_{fd}I_fS_d(1-u_1)}{N_d^2}\end{aligned} \tag{75}$$

$$\begin{aligned}\lambda_4^{'}=&\lambda_4\mu_d-\frac{\lambda_5\beta_{df}b_{fd}I_dS_f}{N_d^2}+\frac{\lambda_6\beta_{df}b_{fd}I_dS_f}{N_d^2}-\lambda_1\left(\rho+\frac{\beta_{fd}b_{fd}I_fS_d(1-u_1)}{N_d^2}\right)\\&+\frac{\lambda_2\beta_{fd}b_{fd}I_fS_d(1-u_1)}{N_d^2}\end{aligned} \tag{76}$$

$$\begin{aligned}\lambda_5^{'}=&-A_3+\lambda_7\mu_2I_f-\lambda_6\left(-\mu_2E_f+\frac{\beta_{df}b_{fd}I_d}{N_d}\right)\\&-\lambda_5\left(m_f-\mu_2S_f-\mu_1-\frac{\beta_{df}b_{fd}I_d}{N_d}-\mu_2N_f+\lambda_f(1-u_2)-r_0u_2\right)\end{aligned} \tag{77}$$

$$\begin{aligned}\lambda_6^{'}=&-A_3-\lambda_7(\mu_2I_f+\tau_f)-\lambda_5(-\mu_2S_f+\lambda_f(1-u_2))\\&-\lambda_6(m_f-\mu_1-\mu_2E_f-\mu_2N_f-\tau_f-r_0u_2)\end{aligned} \tag{78}$$

$$\begin{aligned}\lambda_7^{'}=&-A_3+\lambda_6\mu_2E_f+\frac{\lambda_1\beta_{fd}b_{fd}S_d(1-u_1)}{N_d}-\frac{\lambda_2\beta_{fd}b_{fd}S_d(1-u_1)}{N_d}\\&-\lambda_5(\mu_2S_f+\lambda_f(1-u_2))-\lambda_7(-d_f-m_f-\mu_1-\mu_2I_f-\mu_2N_f-r_0u_2)\\&+\frac{\lambda_8\beta_{fh}b_{fh}S_h(1-u_3)}{N_h}-\frac{\lambda_9\beta_{fh}b_{fh}S_h(1-u_3)}{N_h}\end{aligned} \tag{79}$$

$$\begin{aligned}\lambda_8^{'}=&-\lambda_8\left(\gamma_h-\mu_h+\frac{\beta_{fh}b_{fh}I_fS_h(1-u_3)}{N_h^2}\right)-\frac{\beta_{fh}b_{fh}I_f(1-u_3)}{N_h})\\&-\lambda_9\left(\frac{-\beta_{fh}b_{fh}I_fS_h(1-u_3)}{N_h^2}+\frac{\beta_{fh}b_{fh}I_f(1-u_3)}{N_h}\right)\end{aligned} \tag{80}$$

$$\begin{aligned}\lambda_9^{'}=&-A_1-\lambda_{10}\tau_h-\lambda_9\left(-\tau_h-\mu_h-\frac{\beta_{fh}b_{fh}I_fS_h(1-u_3)}{N_h^2}\right)\\&-\lambda_8\left(\gamma_h+\frac{\beta_{fh}b_{fh}I_fS_h(1-u_3)}{N_h^2}\right)\end{aligned} \tag{81}$$

$$\begin{aligned}\lambda_{10}^{'}=&-A_2-\lambda_{11}\delta_h-\lambda_{10}(-\delta_h-d_I-\mu_h-r_I)-\lambda_{12}r_I\\&-\lambda_8\left(\gamma_h+\frac{\beta_{fh}b_{fh}I_fS_h(1-u_3)}{N_h^2}\right)+\frac{\lambda_9\beta_{fh}b_{fh}I_fS_h(1-u_3)}{N_h^2}\end{aligned} \tag{82}$$

$$\lambda_{11}^{'} = -\lambda_{11}(-d_H - \mu_h - r_H) - \lambda_{12} r_H - \lambda_8 \left(\frac{\beta_{fh} b_{fh} I_f S_h (1-u_3)}{N_h^2} + \gamma_h \right) + \frac{\lambda_9 \beta_{fh} b_{fh} I_f S_h (1-u_3)}{N_h^2} \tag{83}$$

$$\lambda_{12}^{'} = \lambda_{12}\mu_h - \lambda_8 \left(\gamma_h + \frac{\beta_{fh} b_{fh} I_f S_h (1-u_3)}{N_h^2} \right) + \frac{\lambda_9 \beta_{fh} b_{fh} I_f S_h (1-u_3)}{N_h^2} \tag{84}$$

The terminal conditions are

$$\lambda_i(T) = 0 \quad for \quad i = 1, 2, \ldots, 12 \tag{85}$$

Moreover, optimal control strategies u_1^*, u_2^*, u_3^* are given by

$$u_1^* = max \left\{ 0, min \left\{ 1, \frac{(\lambda_2 - \lambda_1)\beta_{fd} b_{fd} I_f S_d}{2B_1 N_d} \right\} \right\} \tag{86}$$

$$u_2^* = max \left\{ 0, min \left\{ 1, \frac{\lambda_5 \lambda_f N_f + r_0(\lambda_5 S_f + \lambda_6 E_f + \lambda_7 I_f)}{2B_2} \right\} \right\} \tag{87}$$

$$u_3^* = max \left\{ 0, min \left\{ 1, \frac{(\lambda_9 - \lambda_8)\beta_{fh} b_{fh} I_f S_h}{2B_3 N_h} \right\} \right\} \tag{88}$$

Proof Adjoint equations and transversality conditions can be obtained using Pontryagin's Maximum Principle such that

$$\lambda_1^{'} = -\frac{\partial H}{\partial S_d}, \quad \lambda_1(T) = 0; \quad \lambda_2^{'} = -\frac{\partial H}{\partial E_d},$$
$$\lambda_2(T) = 0; \ldots, \lambda_{12}^{'} = -\frac{\partial H}{\partial R_h}, \quad \lambda_{12}(T) = 0.$$

The optimal control strategies u_1^*, u_2^*, u_3^* can be solved from the optimality conditions,

$$\frac{\partial H}{\partial u_1} = 0, \quad \frac{\partial H}{\partial u_2} = 0, \quad \frac{\partial H}{\partial u_3} = 0.$$

4.3 Numerical results

We numerically calculated optimal control strategies based on the iterative method used in Blayneh et al. (2010). Given initial state conditions without controls, we solved the state differential equation (55)–(66) forward in time using the fourth order Runge-Kutta method. According to results of state values and the given final value in Eq. (85), we solved adjoint values in Eqs. (73)–(84) backward in time, using the fourth order Runge-Kutta method. Both updates of state values and adjoint values were utilized to calculate optimal control strategies in Eqs. (86)–(88). This process was repeated until a steady state was achieved. This algorithm is given below.

Step 1 Initialize state variables: $S_d(0)$, $E_d(0)$, $I_d(0)$, $R_d(0)$, $S_f(0)$, $E_f(0)$, $I_f(0)$, $S_h(0)$, $E_h(0)$, $I_h(0)$, $H_h(0)$, $R_h(0)$ Initialize optimal control strategies: u_1, u_2, u_3.

Step 2 Given small value $\varepsilon_1, \varepsilon_2, \varepsilon_3$ and final time value T: While change of state values $>\varepsilon_1$, or change of adjoint values $>\varepsilon_2$, or change of controls $>\varepsilon_3$, do:

(i) Solve state values forward in time from 0 to T based on Eqs. (55)–(66), using the fourth order of Runge-Kutta.
(ii) Solve adjoint values backward in time from T to 0 based on Eqs. (73)–(84), using the fourth order of Runge-Kutta.
(iii) Solve control strategies u_1, u_2, u_3 using Eqs. (86)–(88).

Step 3 Find optimal control strategies: $u_1^* = u_1, u_2^* = u_2, u_3^* = u_3$.

The fourth order of Runge-Kutta method adopted here is given below.

$$\frac{dy}{dt} = f(y,t)$$
$$y_{i+1} = y_i + \frac{1}{6}(k_1 + 2k_2 + 2k_3 + k_4)h$$

where

$$k_1 = f(y_i, t_i)$$
$$k_2 = f\left(y_i + \frac{1}{2}k_1 h, t_i + \frac{1}{2}h\right)$$
$$k_3 = f\left(y_i + \frac{1}{2}k_2 h, t_i + \frac{1}{2}h\right)$$
$$k_2 = f(y_i + k_3 h, t_i + h)$$

h is step size, given by $h = t_{i+1} - t_i$.

Parameter used in this section is defined in Table 3. The initialization of dogs, sand flies, and human population is given by $S_d(0) = 100$, $S_f(0) = 10{,}000$, $S_h(0) = 100$, $I_f(0) = 10$, and $I_d(0) = 5$. We proposed that control strategy effectiveness could not be 100 % effective for each strategy; then we reduced the upper bound of each control to observe the impact of control. The upper bounds of each control strategy u_1, u_2, and u_3, were considered as 60, 50, and 60 %, respectively.

Figure 5 describes scenarios for state variables E_h, I_h, and N_f for the case which $A_1 = 1$, $A_2 = 1$, $A_3 = 1e{-}5$, $B_1 = 1$, $B_2 = 1$, and $B_3 = 1$, meaning the reduction of exposed human and infected human are more important than the reduction of number of sand flies and the cost of three control strategies are similar. Optimal control strategies are shown in Fig. 6.

From the result in Fig. 5, the number of exposed humans, infected humans, and infected sand flies were effectively controlled by the corresponding control strategies. However, the cost of each strategy did not have to be equal. When $B_1 = 100$, $B_2 = 1$, and $B_3 = 3$, meaning the dogs prevention measurement costs more, the control strategies are changed correspondingly. Figure 7 illustrates control strategies u_1, u_2, and u_3 in this scenario.

Table 3 Parameter values in numerical analysis

Parameters	Values	References
λ_d	0.02	Assumed
λ_f	0.05	Assumed
λ_h	0.05	Blayneh et al. (2010)
$1/\mu_d$	700	Hartemink et al. (2011)
$1/\mu_h$	12000	Blayneh et al. (2010)
b_{fd}	0.1	Hartemink et al. (2011)
b_{fh}	0.1	Hartemink et al. (2011)
β_{fd}	0.5	Hartemink et al. (2011)
β_{df}	0.7	Hartemink et al. (2011)
β_{fh}	0.5	Hartemink et al. (2011)
d_d	0.01	Hartemink et al. (2011)
d_f	0	Assumed
d_I	0.0067	Stauch et al. (2011)
d_H	$3e{-}4$	Stauch et al. (2011)
m_f	$1e{-}4$	Assumed
$1/\tau_d$	10	Hartemink et al. (2011)
$1/\tau_f$	6	Stauch et al. (2011)
$1/\tau_h$	60	Stauch et al. (2011)
δ_h	0.8	Assumed
r_d	0.01	Hartemink et al. (2011)
r_I	0.12	Stauch et al. (2011)
r_H	0.95	Stauch et al. (2011)
ρ	$1e{-}3$	Assumed
μ_1	0.02	Hartemink et al. (2011)
μ_2	$5e{-}6$	Assumed
r_0	0.2	Assumed
γ_h	$2.85e{-}3$	Blayneh et al. (2010)

As the increase of the cost of u_1, the optimal strategies are changed. The strategy for dog disease preventions was adopted much less than previous scenario, shown in Fig. 7a. It is reasonable because increased costs lead to decreased use in order to minimize our objective function. Use of u_2 and u_3 also decreases after around 100 days. From Fig. 8a, b, the number of exposed humans and infected humans both increase slightly due to the lower use of three strategies, while the number of sand flies keeps the same which is shown in Fig. 8c. Hence, the change of the cost of implementing first strategy impacts controlling the number of exposed humans and infected humans but the number of sand flies.

Similarly, the impacts of u_2 and u_3 are evaluated through changing the cost of each strategy, which is shown in Figs. 9, 10, 11 and 12. Compared to the first strategy, the second strategy has the similar impact to the system, as shown in Figs. 9 and 10. The use of u_2 decreases when its cost changes from 1 to 100. Meanwhile, the use of u_1 and

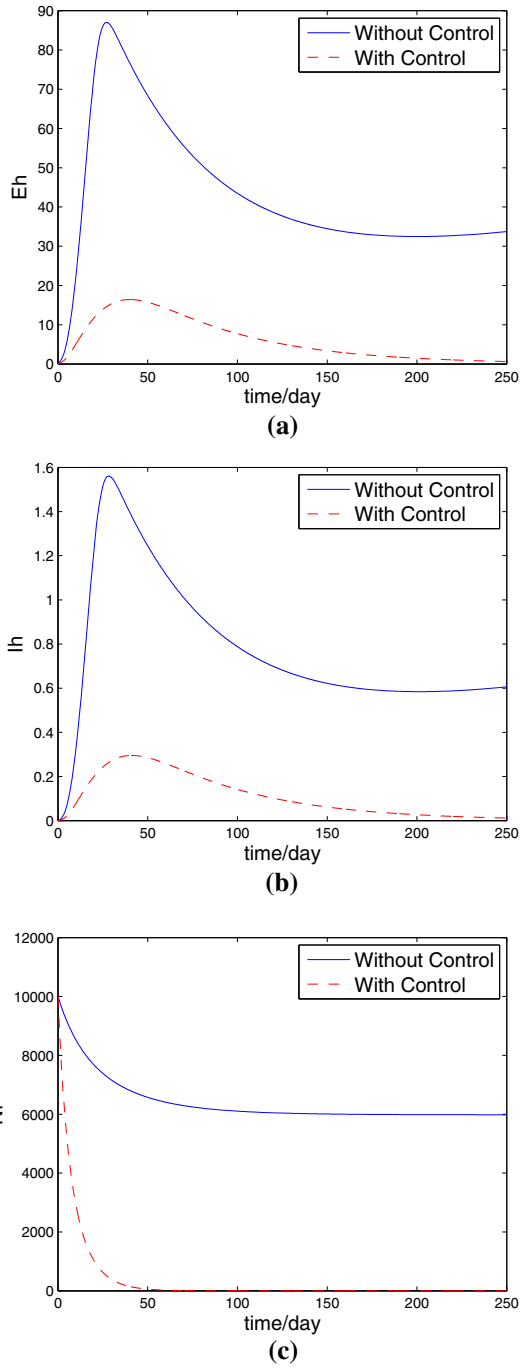

Fig. 5 Simulation with $A_1 = 1$, $A_2 = 1$, $A_3 = 1e{-}5$, $B_1 = 1$, $B_2 = 1$, and $B_3 = 1$

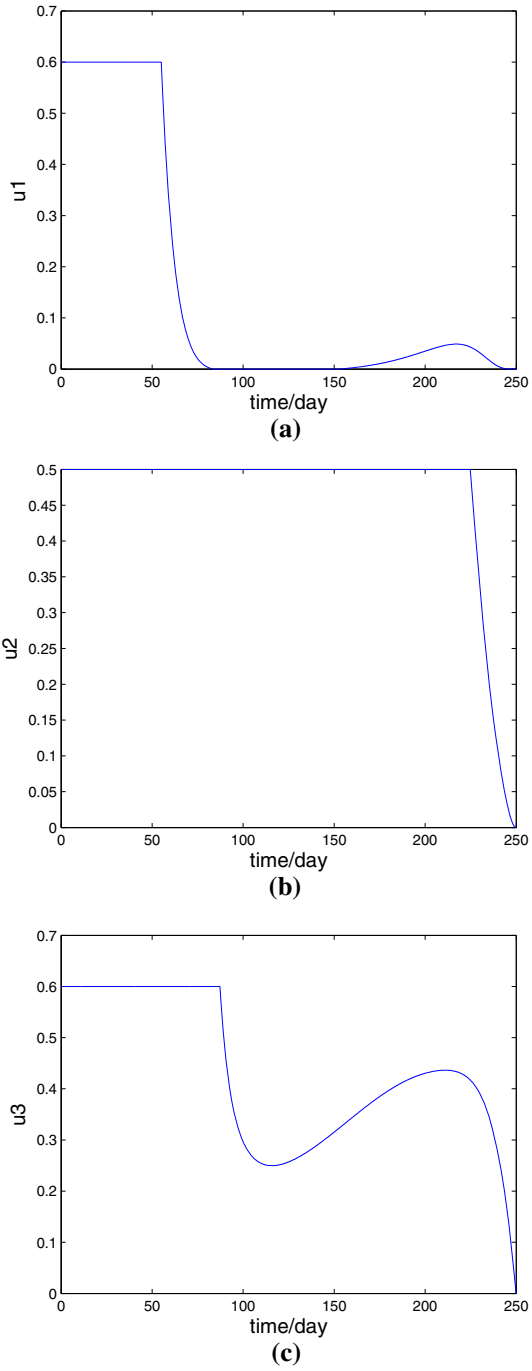

Fig. 6 Control strategies with $A_1 = 1$, $A_2 = 1$, $A_3 = 1e{-}5$, $B_1 = 1$, $B_2 = 1$, and $B_3 = 1$

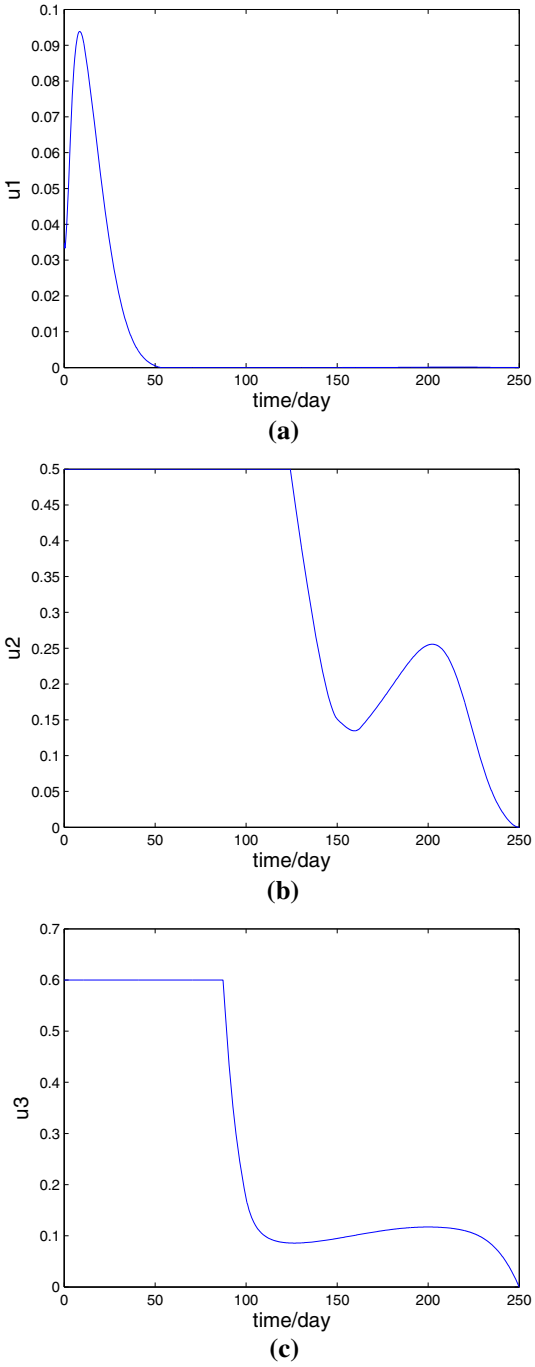

Fig. 7 Control strategies with $A_1 = 1$, $A_2 = 1$, $A_3 = 1e{-}5$, $B_1 = 100$, $B_2 = 1$, and $B_3 = 1$

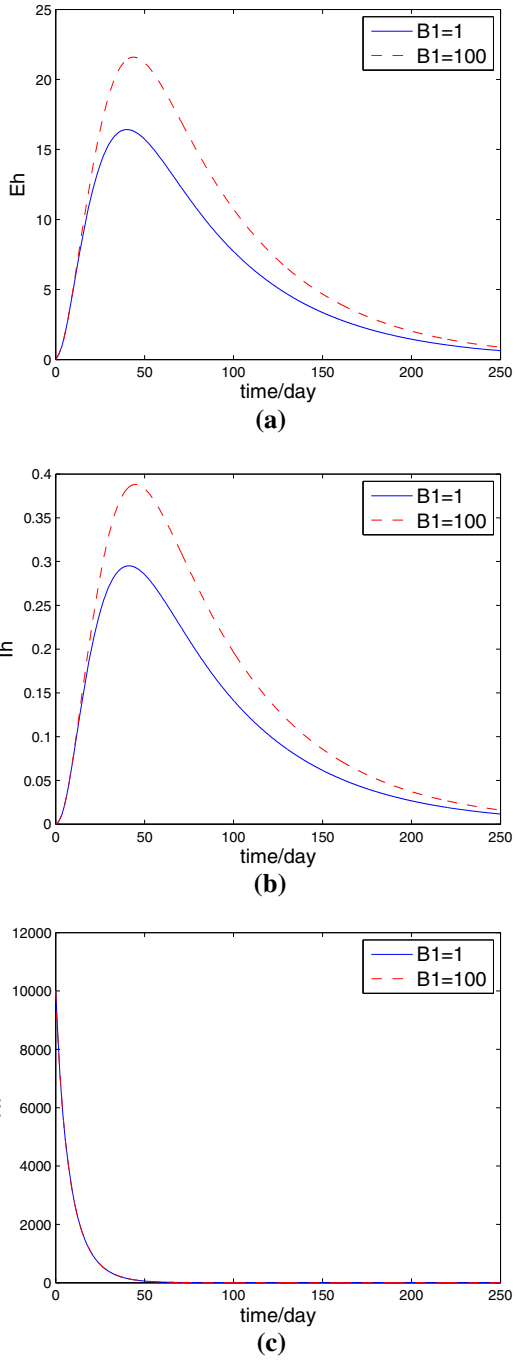

Fig. 8 Simulation with $A_1 = 1$, $A_2 = 1$, $A_3 = 1e{-}5$, $B_2 = 1$, and $B_3 = 1$

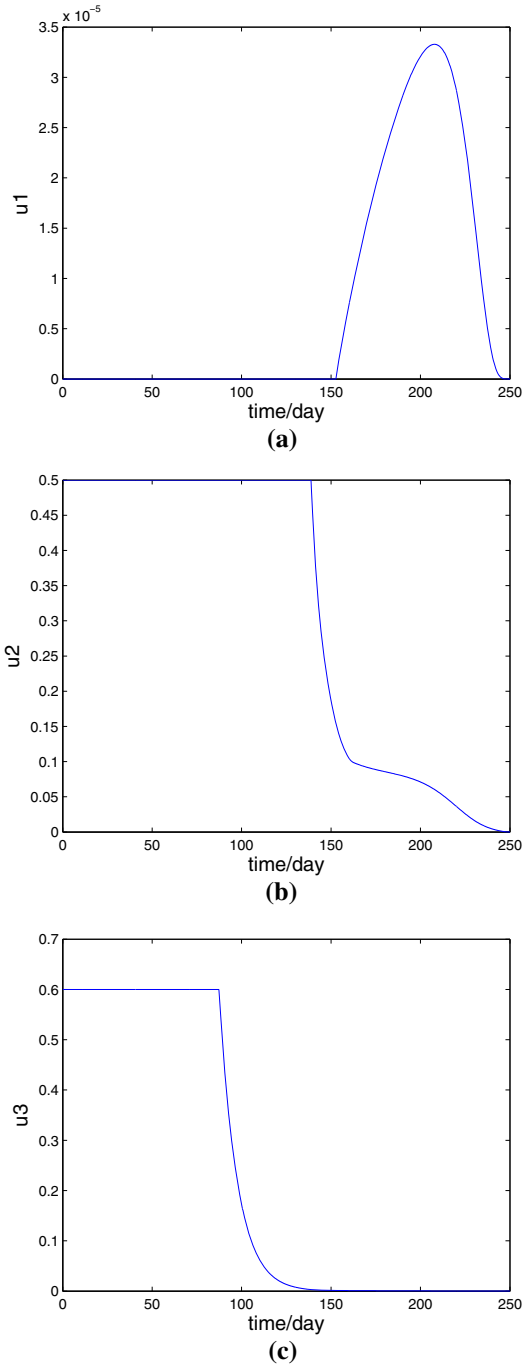

Fig. 9 Control strategies with $A_1 = 1$, $A_2 = 1$, $A_3 = 1e{-}5$, $B_1 = 1$, $B_2 = 100$, and $B_3 = 1$

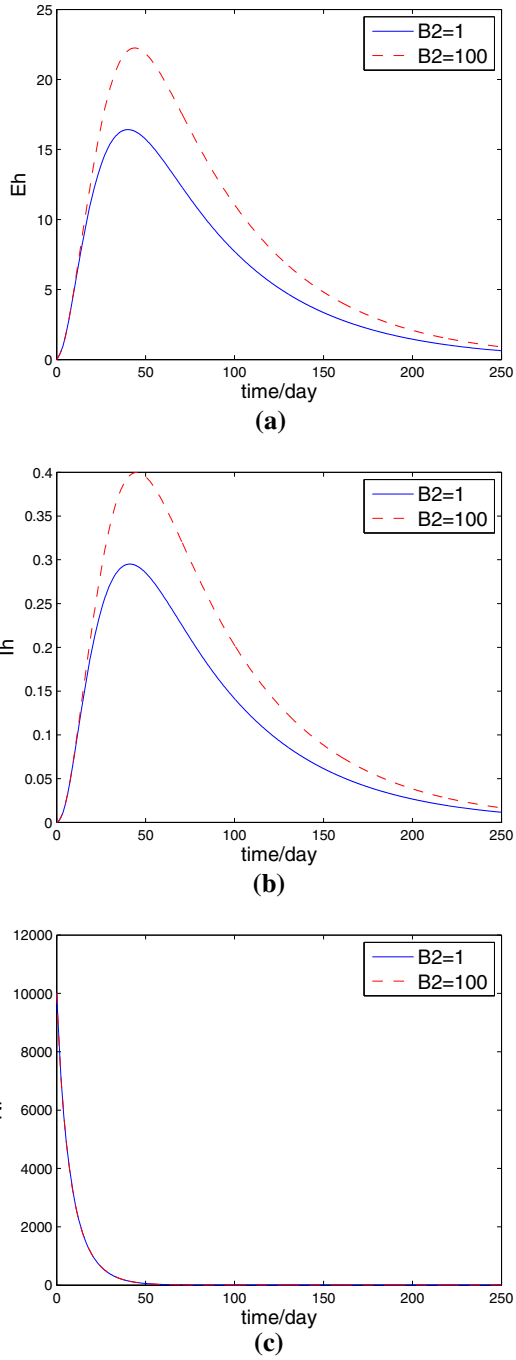

Fig. 10 Simulation with $A_1 = 1$, $A_2 = 1$, $A_3 = 1e{-}5$, $B_1 = 1$, and $B_3 = 1$

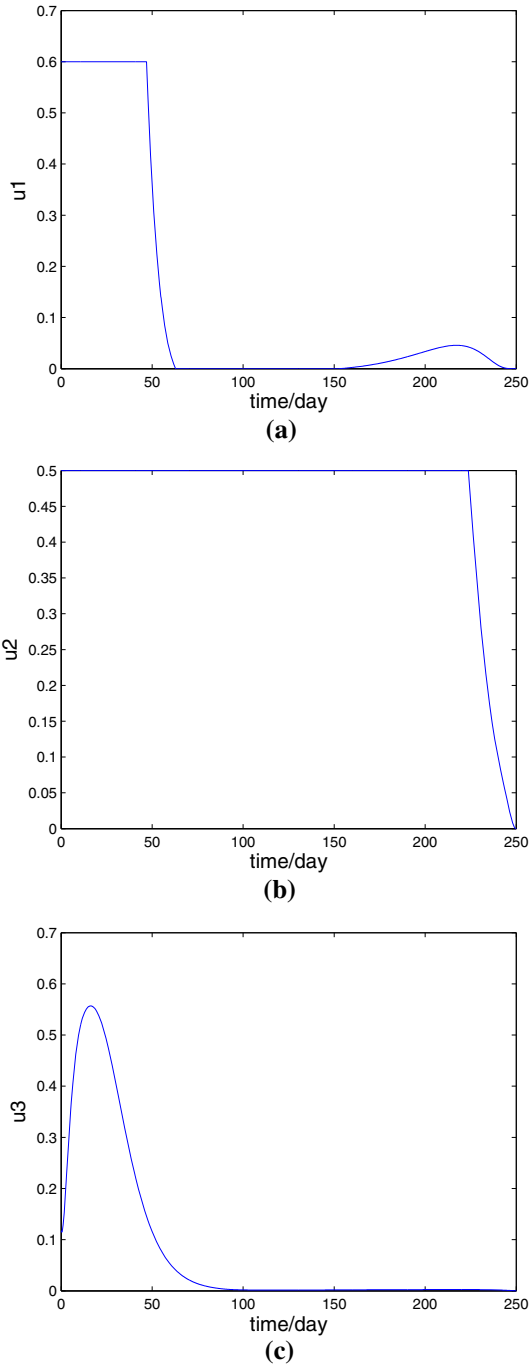

Fig. 11 Control strategies with $A_1 = 1$, $A_2 = 1$, $A_3 = 1e{-}5$, $B_1 = 1$, $B_2 = 1$, and $B_3 = 100$

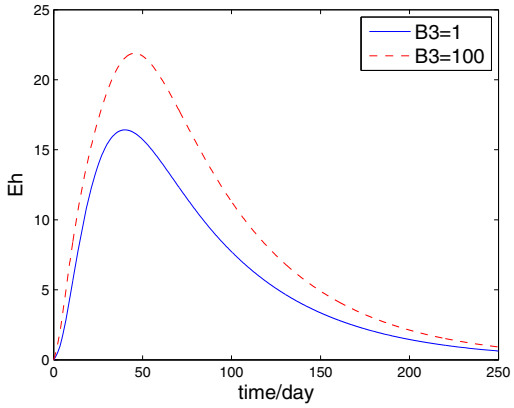

(a)

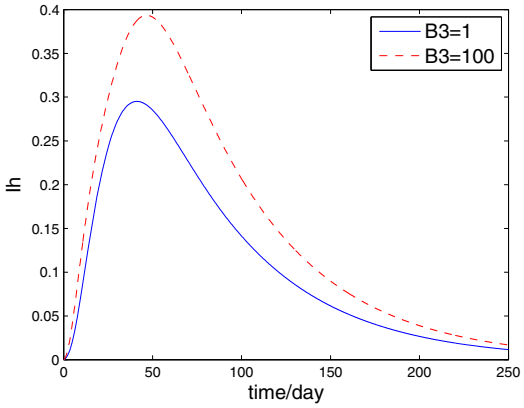

(b)

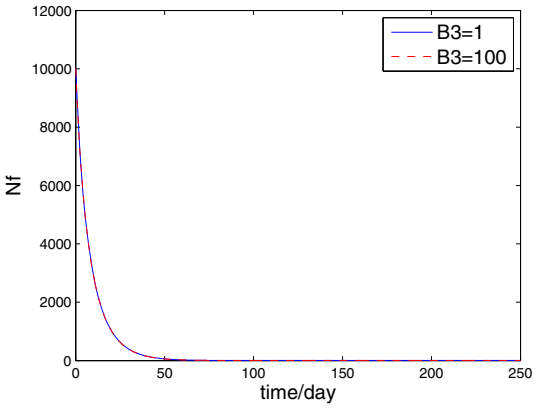

(c)

Fig. 12 Simulation with $A_1 = 1$, $A_2 = 1$, $A_3 = 1e{-}5$, $B_1 = 1$, and $B_2 = 1$

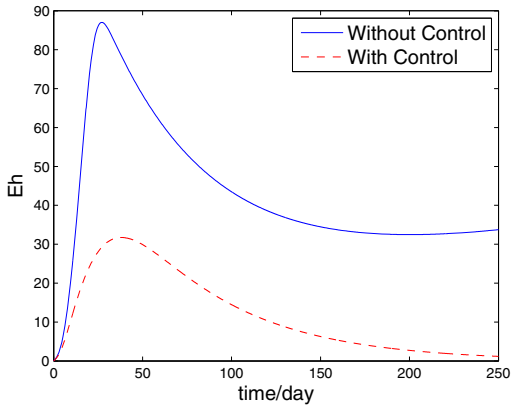

(a)

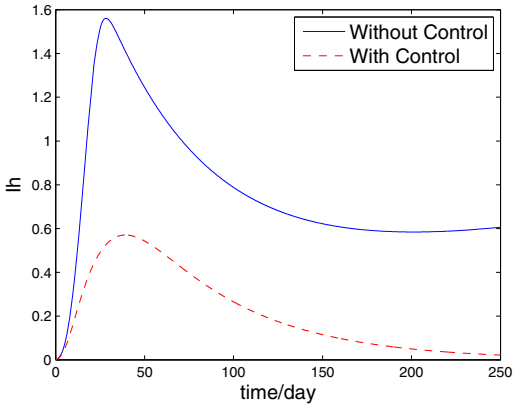

(b)

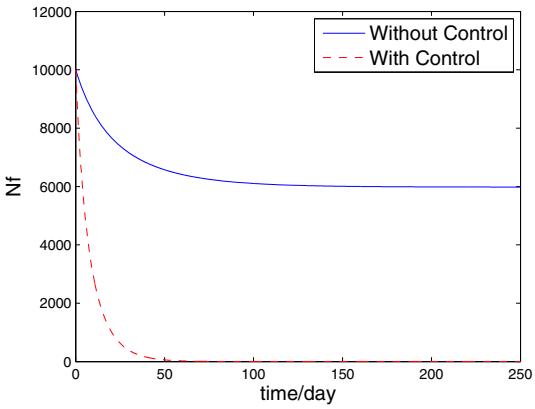

(c)

Fig. 13 Simulation with upper bound of control $u_3 = 0.1$

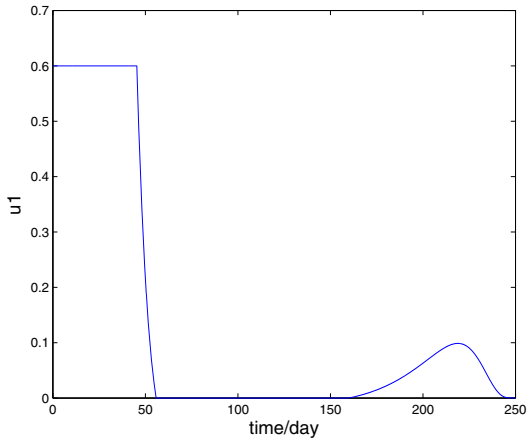

(a)

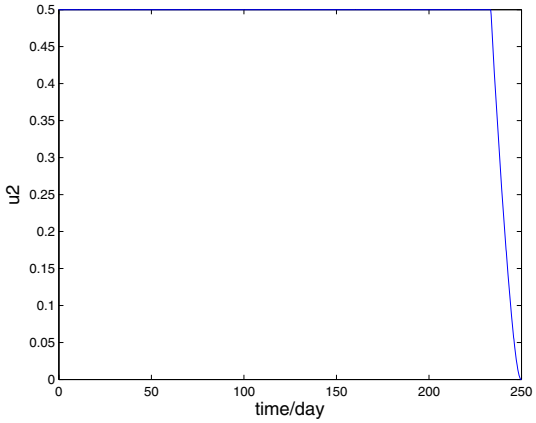

(b)

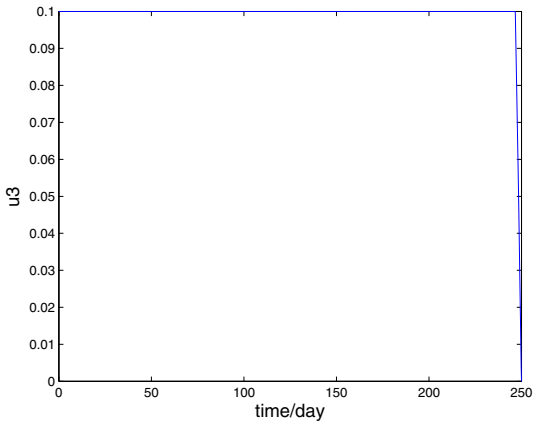

(c)

Fig. 14 Simulation with upper bound of control $u_3 = 0.1$

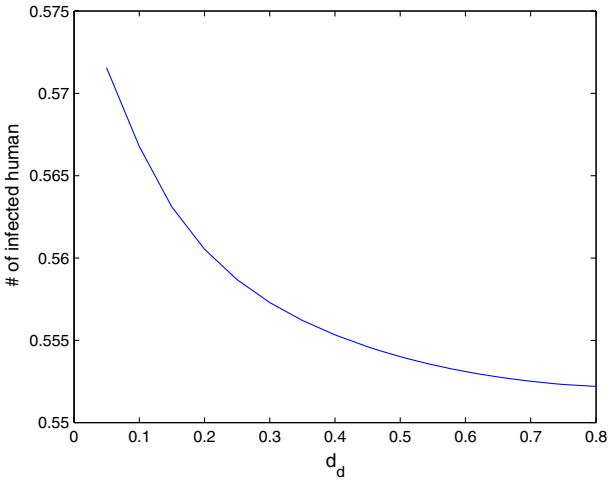

Fig. 15 Sensitivity analysis of culling dog strategy

u_3 also decrease. As a response, the number of exposed humans and infected humans increase and the number of sand flies remains the same.

In Figs. 11 and 12, it shows the impact of changing the cost of the third strategy. As the cost increase from 1 to 100, the use of u_3 is reduced, while the use of u_1 and u_2 keep the same. As a result, it leads to more exposed humans and infected humans and the number of sand files remains the same.

In sum, the overall use of the corresponding strategy decreases leading to the increased number of exposed and possibly infected humans, as the estimated cost for disease prevention in dogs, sand flies, and humans increase. Further, our simulation (presented in Figs. 8, 10, and 12) indicate that the number of sand flies does not change significantly as the cost of the control strategies increase, whereas the number of exposed and infected humans increase. This indicates that the number of sand flies has a greater impact for minimizing our objective function. To control the number of sand flies, the use of u_2 (i.e., insecticide used to control sand flies) has to remain at high level. This is supported by our simulations of (unchanged) insecticide use for the first 150 days even if the cost of insecticides increases from 1 to 100 (Figs. 7, 9, 11). Taken together, our results indicate that controlling the number of sand flies is the most effective and recommended methodology to control ZVL transmission.

In addition, change of effectiveness of control strategies impacts the dynamics of the entire system from Eqs. (55)–(66). Let upper bound of $u_3 = 0.1$, meaning that the effectiveness of human prevention from disease is extremely low. The number of exposed human, infected human, and infected sand fliessand flies are depicted in Fig. 13. Compared to Fig. 5, an increasing number of exposed and infected human populations is evident in Fig. 13 due to the lessened control strategy effectiveness of prevention measurement for humans. In Fig. 14, the use of each control strategy is shown and there is no big difference for the use of the first strategy and the second strategy.

Based on the above analyses, it is shown that control of ZVL transmission using the three strategies (u_1, u_2, u_3) is doable. In addition to the above strategies, culling dogs is often adopted as a control strategy for ZVL. Although culling dogs has been used, its efficacy has frequently been questioned. Our analysis of the parameter d_d, [in Eq. (57)] especially when the other three approaches are not available, clearly show culling to be ineffective (Fig. 15), regardless of the culling rate.

5 Conclusion

Here, a three-system mathematical model for ZVL transmission with dogs, sand flies, and humans, was developed using a modified SEIR model. Backward bifurcation analysis suggested that $R_0 < 1$ is not a sufficient condition to control the spread of disease in this model, and both disease-free equilibrium and endemic equilibrium can coexist under certain conditions. Therefore, the condition $R_0 < R_c$ is required in order to control or eradicate the disease. A specific mathematical method to calculate optimal control strategies was given in this paper. Pontryagins maximum principle, previously used to identify optimal control strategies against West Nile (Blayneh et al. 2010) or other vector-borne diseases (Lashari et al. 2013), was also used here to determine possible optimal control strategies for ZVL. The results obtained for optimal control were highly dependent on the cost of each strategy and the effectiveness of each control strategy. Interestingly, our results (optimal system analysis) suggest that as the estimated cost for disease prevention increases, the overall use of the corresponding strategy or strategies decreases leading to the increased number of exposed and possibly infected humans. Further, our simulation (presented in Figs. 8, 10, 12) indicate that the number of sand flies does not change significantly as the cost of the control strategies increase, whereas the number of exposed and infected humans increase. This indicates that the number of sand flies has a greater impact for minimizing our objective function. To control the number of sand flies, the use of u_2 (i.e., insecticide used to control sand flies) has to remain at high level. This is supported by our simulations of (unchanged) insecticide use for the first 150 days even if the cost of insecticides increases from 1 to 100 (Figs. 7, 9, 11). Taken together, our results indicate that controlling the number of sand flies is the most effective and recommended methodology to control ZVL transmission. Culling dogs is not an effective strategy to control the disease transmission. Although the simulation result shows ZVL may be controlled effectively adopting the corresponding control strategies, the parameter $A_1, A_2, A_3, B_1, B_2, B_3$ used in the objective function are quite subjective. Therefore, further studies will focus on validation of the model in terms of real data and on actual control costs and effectiveness in various scenarios, especially for different endemic areas of ZVL.

Compliance with ethical standards

Conflict of interest The authors declare no competing interests.

Human and animal participants No humans or animals were used in the course of this study.

References

Blayneh KW, Gumel AB, Lenhart S, Clayton T (2010) Backward bifurcation and optimal control in transmission dynamics of west nile virus. Bull Math Biol 72(4):1006–1028

Burattini MN, Coutinho FA, Lopez LF, Massad E (1998) Modelling the dynamics of leishmaniasis considering human, animal host and vector populations. J Biol Syst 6(04):337–356

Castillo-Chavez C, Song B (2004) Dynamical models of tuberculosis and their applications. Math Biosci Eng 1:361–404

Chappuis F, Sundar S, Hailu A, Ghalib H, Rijal S, Peeling RW, Alvar J, Boelaert M (2007) Visceral leishmaniasis: what are the needs for diagnosis, treatment and control? Nat Rev Microbiol 5(11):873–882

Courtenay O, Quinnell RJ, Garcez LM, Shaw JJ, Dye C (2002) Infectiousness in a cohort of brazilian dogs: why culling fails to control visceral leishmaniasis in areas of high transmission. J Infect Dis 186(9):1314–1320

Dantas-Torres F, Brandão-Filho SP (2006) Visceral leishmaniasis in brazil: revisiting paradigms of epidemiology and control. Revista do Instituto de Medicina Tropical de São Paulo 48(3):151–156

Desjeux P (2004) Leishmaniasis: current situation and new perspectives. Comp Immunol Microbiol Infect Diseases 27(5):305–318

Fleming W, Rishel R (1975) Deterministic and stochastic optimal control. Springer, New York

Garba SM, Gumel AB, Bakar MA (2008) Backward bifurcations in dengue transmission dynamics. Math Biosci 215(1):11–25

Hartemink N, Vanwambeke SO, Heesterbeek H, Rogers D, Morley D, Pesson B, Davies C, Mahamdallie S, Ready P (2011) Integrated mapping of establishment risk for emerging vector-borne infections: a case study of canine leishmaniasis in southwest france. PLoS One 6(8):e20,817

Jamjoom M, Ashford R, Bates P, Chance M, Kemp S, Watts P, Noyes H (2004) Leishmania donovani is the only cause of visceral leishmaniasis in east africa; previous descriptions of l. infantum and l. archibaldi from this region are a consequence of convergent evolution in the isoenzyme data. Parasitology 129(04):399–409

Kedzierski L, Zhu Y, Handman E (2006) Leishmania vaccines: progress and problems. Parasitology 133(S2):S87–S112

Keeling MJ, Rohani P (2008) Modeling infectious diseases in humans and animals. Princeton University Press, Princeton

Lashari AA, Hattaf K, Zaman G, Li XZ (2013) Backward bifurcation and optimal control of a vector borne disease. Appl Math 7(1):301–309

Pontryagin LS (1987) Mathematical theory of optimal processes. CRC Press, Boca Raton

Ramiro MJ, Zárate JJ, Hanke T, Rodriguez D, Rodriguez JR, Esteban M, Lucientes J, Castillo JA, Larraga V (2003) Protection in dogs against visceral leishmaniasis caused by leishmania infantum is achieved by immunization with a heterologous prime-boost regime using dna and vaccinia recombinant vectors expressing lack. Vaccine 21(19):2474–2484

Ribas LM, Zaher VL, Shimozako HJ, Massad E (2013) Estimating the optimal control of zoonotic visceral leishmaniasis by the use of a mathematical model. Sci World J

Rosypal AC, Zajac AM, Lindsay DS (2003) Canine visceral leishmaniasis and its emergence in the united states. Vet Clin North Am 33(4):921–937

Smith HL (2008) Monotone dynamical systems: an introduction to the theory of competitive and cooperative systems, vol 41. American Mathematical Society, USA

Stauch A, Sarkar RR, Picado A, Ostyn B, Sundar S, Rijal S, Boelaert M, Dujardin JC, Duerr HP (2011) Visceral leishmaniasis in the indian subcontinent: modelling epidemiology and control. PLoS Negl Trop Diseases 5(11):e1405

Van den Driessche P, Watmough J (2002) Reproduction numbers and sub-threshold endemic equilibria for compartmental models of disease transmission. Math Biosci 180(1):29–48

Zhang W, Wahl LM, Yu P (2014a) Modeling and analysis of recurrent autoimmune disease. SIAM J Appl Math 74(6):1998–2025

Zhang W, Wahl LM, Yu P (2014b) Viral blips may not need a trigger: how transient viremia can arise in deterministic in-host models. SIAM Rev 56(1):127–155